LENS CRYSTALLINS: USE IN TISSUE ENGINEERING APPLICATIONS AND DRUG DELIVERY STRATEGIES

A Thesis submitted in partial fulfilment of the requirements for the degree of

Master of Technology
In
Biotechnology
By

Priyanka Goyal
213BM2023

Under The Supervision of

Prof. Sirsendu Sekhar Ray

And Co-Supervision of

Prof. Kunal Pal

Department of Biotechnology & Medical Engineering
National Institute of Technology
Rourkela-769008, Orissa, India
May, 2015

National Institute of Technology, Rourkela

CERTIFICATE

This is to certify that the thesis entitled "**Lens crystallins: use in tissue engineering applications and drug delivery strategies**" by **PRIYANKA GOYAL (213BM2023)** submitted to the National Institute of Technology, Rourkela for the award of Master of Technology in Biotechnology during the session 2013-2015 is a record of bonafide research work carried out by her in the Department of Biotechnology and Medical Engineering under my supervision and guidance.

To the best of my knowledge, the matter embodied in the thesis has not been submitted to any other University / Institute for the award of any Degree or Diploma.

Prof. Sirsendu Sekhar Ray
Assistant Professor
Department of Biotechnology & Medical Engineering
National Institute of Technology
Rourkela-769008

ACKNOWLEDGEMENT

For the successfully completion of this project many people have been important and without acknowledging them this project will remain incomplete. So first of all I would like to thank **God** and my parents **Mr. Mahesh Goyal** and **Mrs. Vinita Goyal** for their blessings.

I would like to express my deep gratitude towards my project supervisor **Dr. Sirsendu Sekhar Ray** and my co-supervisor **Dr. Kunal Pal**, for their guidance, advice, motivation and support throughout my project.

I am highly obliged and grateful to **Dr. Krishna Pramanik**, HOD, Department of Biotechnology and Medical engineering, for providing me the opportunity, support and the guidance for this project.

I would also like to thank **Mr. Rik Dhar, Mr. Joseph Christakiran, Mr. Narendra Babu, Miss Alisha Prasad, Miss Abinaya, Miss Sweta Naik, Mr. Uvanesh K., Mr. Gauri Shankar Shaw, Mr. Senthil Guru** and **Mr. Deependra Ban** for their invaluable help and support in this project.

I want to express my special thanks to **Department of Chemistry**, **Department of Life Science** and other departments for providing me their infrastructure and the facilities without which this project wouldn't have been possible.

CONTENTS

ABSTRACT

The current study describes about the use of lens protein crystallins in tissue engineering applications as well as its role in drug delivery strategies. To show their tissue engineering applications, these structural proteins were tried to be fabricated into nanofibers by the process of electrospinning. For the preparation of electrospin fibers, first the crude mixtures of the lens protein solution were lyophilized and made into powder and these were then compared to each other on the basis of their structural changes and activity by doing characterizations like SDS-PAGE, FTIR spectroscopic study, circular dichroism, chaperone activity study. The results showed no such significant differences between the lens proteins before and after lyophilization. Further, these lyophilized powder were mixed with different solvents and finally it was found that with 40% protein/TFA solution the proteins are getting electropun nicely and proper nanofibers were prepared. The morphology of the prepared fibers were then studied using Scanning electron microscope (SEM) and the diameters of these were found to be in nanometer range. These fibers were then compared with the lyophilized lens powder using FTIR spectroscopic study, XRD, solubility study and the changes between the two were analyzed. The FTIR spectroscopic study and the XRD study of the nanofibers showed the characteristics of an amyloid fibril formation. Further to analyze the biocompatible nature of the electrospun fibers cytocompatibility and cell proliferation studies were done. The fibers were found to be biocompatible in nature. To show the role of these protein in drug delivery strategies a dual environment responsive hydrogels were prepared as a model system. These were successfully synthesized and characterized using XRD, FTIR, swelling mechanical, electrical and *in vitro* studies. Drug delivery kinetics study using insulin was done to see if these hydrogels can deliver drug in a sustained way or not and thus can be used successfully as a model system with crystallins.

Keywords: crystallin, electrospinning, hydrogels, protein drug delivery, amyloid fibrils

LIST OF TABLES

LIST OF FIGURES

1 INTRODUCTION

Eye lens is a soft, avascular, transparent, highly structured tissue whose crucial function is to focus light on to the retina. The refractive properties of the eye lens and maintenance of its transparency is highly dependent on the well-ordered structural proteins in the eye lens called the crystallins [1]. More than 90% of the total dry mass of the lens is made up of crystallins and there are in general three classes of lens crystallins: α, β, γ, which are found in the mammalian lens. Each class of crystallin constitutes one-third of the total mass of the lens protein, major being the α-crystallin. α-crystallin consists of two genes: αA and αB in the ratio of 3:1 and is found as a heterogeneous multimeric complex having molecular weight distribution from 300 kDa to 1 million, with each monomer having an average size of 20 kDa [2]. In addition to the structural role of these proteins, in 1992 it was first shown that α-crystallin has chaperone-like function [3] which prevents the formation of large light-scattering aggregates and cataracts by binding to the unfolded or denatured proteins of other crystallins (β and γ crystallins, including itself). Since then, detailed study on α-crystallins have been carried out and many novel functions of these in the lens and other parts of the eye have been identified. The novel functions of the α-crystallin include, anti-apoptotic function, its role in retinal and choroidal angiogenesis through interaction with vascular endothelial growth factor, anti-inflammatory effect, have neuroprotective role, etc. The genetic and biochemical studies have also implicated their role in cancers. In addition to these, many research have been going on with other types of lens crystallin proteins, such as, β and γ crystallins and it has been found out by Zhang *et al*. that these proteins have potential role in the vascular remodeling of the eye in the presence of the vascular endothelial growth factor [4]**.** The crystallins also have shown the propensity to form amyloid fibrils (highly ordered structures) thereby showing its

possible applications in the emerging field of bionanomaterials and tissue engineering applications [5].

Taking inspiration from the above mentioned novel functions of the lens crystallin that have been found in the recent years, especially their role in angiogenesis and neuroprotection as well as their role in vascular remodeling, we proposed that these proteins can be effectively used in the tissue engineering applications. In addition to this, due to their role as a molecular chaperone, we hypothesized that these can help in the suppression of the non-specific irreversible aggregation of the proteins and thus help in maintaining the stability of the proteins, during their delivery through a polymeric system, such as, hydrogels, organogels etc.

In order to see their role in tissue engineering applications, crude mixtures of these proteins were lyophilized and made into powder form. These lyophilized powder were then compared with the crude lens solution prepared previously, on the basis of their structural as well as functional properties by using characterization techniques, such as, SDS-PAGE, FTIR spectroscopic study, circular dichroism study, ANS fluorescence study, and to check their functional properties, chaperone activity studies were done. After this, these lyophilized powder were then tried to be fabricated into nanofibers in order to be used for tissue engineering purposes by the process of electrospinning. After optimizing the electrospinning process and successfully electrospinning these proteins into fibers, a comparison of these with the lyophilized lens powder were made by using techniques like FTIR spectroscopic study, XRD study, solubility study etc. The biocompatibility of the prepared fibers as well as the lyophilized lens powder were done by doing cytocompatibility and cell proliferation studies using Adipose derived stem cells (ADSCs). The lyophilized lens powder as well as the fibers were found to be biocompatible.

For the purpose of showing the role of these proteins in drug delivery strategies, first a model system was prepared through which the sustainable protein drug delivery was supposed to be attained. Hydrogels were chosen as the model system, as it is considered to be the polymeric constructs that has the ability to absorb as well as retain water within its structure. Also, from long time hydrogels have been used for designing various biomedical products, e.g. drug delivery matrices, tissue engineering scaffolds, etc. In the last decade, there has been a great interest in designing stimuli-responsive hydrogels [6]. This is because of the fact that these hydrogels have shown a great potential in controlled delivery and tissue engineering applications.

Therefore, by utilizing the pH sensitive behavior of Poly (2-hydroxyethylmethacrylate) (pHEMA) which was first used for synthesizing hydrogels for biomedical applications, in the year of 1960 [7] and by exploring the temperature sensitive behavior of the methyl cellulose (MC), we hypothesized that novel dual environment responsive hydrogels can be obtained by preparing semi-IPN hydrogels of pHEMA and MC. Thus an attempt was made to develop the dual-environment responsive hydrogels which may have wide biomedical applications, such as, controlled drug release, thermos chemotherapy, etc. HEMA was cross-linked using free radical polymerization, whereas, MC was not cross-linked. The developed hydrogels were thoroughly characterized by FTIR spectroscopy, XRD and mechanical studies. The environment sensitive behavior of the semi-IPN hydrogels was studied by conducting swelling studies at different pH and temperature conditions. Further, to ascertain the biocompatible nature of the hydrogels cyto-compatibility test was conducted using HaCaT cells. Also, to see whether the proteins are being delivered effectively and efficiently from the prepared hydrogels system, insulin drug delivery kinetics study was carried out and the drug delivery efficiency of the prepared system was found out.

2 OBJECTIVES

For Tissue Engineering Purposes

- To characterize the lyophilized crude lens and its comparison with the lens solution before lyophilization
- Optimizing the electrospinning process and electrospinning of the lyophilized crude lens
- Comparison between the lyophilized powder and the electrospunned fibers of the crude lens

For Drug Delivery strategies

- To fabricate dual environment responsive hydrogel system for sustainable drug delivery
- To characterize dual responsive hydrogel system for crystallin stable sustainable insulin delivery

3 LITERATURE SURVEY

The most important of all senses is the vision. The crucial part of this being the eye lens whose main role is to focus light on to the retina. The lens is highly dependent on the well-ordered arrangement of the crystallin proteins to maintain its transparency. The crystallin proteins are the major structural proteins that are found in the eye lens and it makes up to 90% of the total dry weight of the lens. There are basically three types of crystallin proteins: α, β, and γ crystallin, the major of which being the α-crystallin which constitutes up to 40 % of the total mass of the lens proteins. It was described by Morner in 1894 that apart from these three major proteins lens have other distinct proteins too [8]. This was further showed by Wood, Massi, and Solomon [9] in their work with rabbit lens homogenates, where they crystallized five proteins from their homogenates. Since then extensive research has been going on the individual lens crystallin proteins and many novel functions have been found out. It was first shown in 1992 by J. Horwitz that apart from the structural roles of the lens α-crystallins, they show chaperone like properties and thus play a functional role too in the eye. After this finding, detailed study on these proteins were carried out and it was found that these protein show anti-apoptotic function, shows angiogenic functions in retina and choroids with their interaction with the vascular endothelial growth factor (VEGF) [10] [11], has anti-inflammatory function [12] [13] [14] [15]**,** have neuroprotective effects [16] [17], etc. The genetic and biochemical studies have also implicated their role in cancers. The anti-inflammatory function of the crystallin proteins was first described by Masilmoni in mice [13]**.** Also it was shown by Dimberg *et al* that α-crystallins promotes tumor angiogenesis by increasing the endothelial cells survival during tube morphogenesis. Thus these were shown to be novel class of angiogenic modulators. Not only α-crystallins but recently in the year 2005 Zhang *et al* showed

that β and γ crystallins also have potential role in vacular remodeling of the eye in the presence of VEGF.

The angiogenic and vascular remodeling function of the crystallin proteins were shown using knocked out models in mouse, where it was seen that removal of these proteins resulted in attenuation of neovascularization, whereas, the wild type showed prominent neovascularization. The role of the crystallins towards angiogenesis and vasculogenesis depends on the cell and the tissue type and occurs through multiple mechanisms. These proteins can act directly and/or indirectly on the endothelial cells and other cell types such as retinal pigmented epithelium (RPE). On the other hand, the chaperone activity of the crystallin proteins were shown under *in vitro* experimental conditions using bovine α-crystallin for the first time. These proteins showed suppression of aggregation of several enzymes, as well as prevented the heat induced aggregation of β and γ crystallins including itself. The mechanism of this chaperone function shown by the crystallin proteins has been studied by many researchers and it was out that there are many binding sites, present in each oligomer of α-crystallin, for the substrates to bind to. The substrates that are binding to these sites are found to be in the molten globular state. [18] [19]. Also it was found out that the major determinants that regulate the interaction of a protein with molecular chaperones are supposed to be the kinetic factors. Therefore seeing its role in angiogenesis and vasculogenesis as well as their function as a molecular chaperone it was proposed by us that we can use the crude mixtures of the lens protein crystallins for their application in bionanomaterials as well as in tissue engineering purposes. Also we proposed that maybe we can utilize the chaperone properties of these proteins during sustainable drug delivery of the proteins and thus avoid the unwanted aggregation of the proteins inside the system through which it is delivered. Also it was thought that these proteins can help in not only preventing the aggregation of the proteins inside the

delivery system but also stabilize the protein in the system for a longer time before they are actually being delivered from the system. The first objective was targeted by the process of electrospinning through which fibers of these structural proteins were tried to be fabricated so that these can be used as a novel bionanomaterial as well as for other tissue engineer applications.

Electrospinning is a process which utilizes electrical forces to produce protein or polymer fibers having diameters ranging from 2 nm to several micrometers, using protein as well as polymer solutions of both naturally and synthetically produced proteins and/or polymers. Thus by utilizing this process nanofibers of these lens proteins were made for the first time and thus all the necessary characterizations were done. It was shown that these proteins can actually be used as a bionamaterial as well as in tissue engeering application.

In order to target the second objective, hydrogels were prepared as a model system. Hydrogels were chosen as it has the ability to absorb and retain water in its structure. As it is believed that stimuli responsive hydrogels are better and have the potential to be used in controlled drug delivery as well as other biomedical applications. For this purpose, poly (hydroxyethyl methacrylate) (pHEMA) was chosen which has been used for long time to prepare soft contact lenses. It has been shown in literatures that these pHEMA shows pH sensitivity and thus have good mechanical properties. Also it has been shown previously that the pHEMA hydrogels are biocompatible in nature. These hydrogels have also showed high drug loading capacity, higher degree of flexibility and non-toxic nature. Thus due to the above mentioned properties that have been found in the pHEMA hydrogels prepared with different other polymers, such as, dextrin, gelatin etc., this polymer was chosen. Again, to show temperature sensitive behavior of the hydrogels methyl cellulose was chosen as the other polymer with which the hydrogels were made. It was seen from the literatures that methyl cellulose has temperature sensitive behavior and when mixed with other

polymers it has been shown to show thermal responsive behaviors. Also these methyl cellulose hydrogels were found to be non-toxic and non-allergic. The methyl cellulose hydrogels that have been prepared previously have also shown enzyme resistant behavior, low stickiness and high consistency. It is for these reasons we thought of using the individual properties of these polymers and thus making a stimuli responsive hydrogels for the sustainable delivery of the proteins and therefore using this hydrogel system for the crystallin stablized delivery of the proteins.

4 LENS CRYSTALLINS: USE IN TISSUE ENGINEERING APPLICATIONS

4.1 MATERIALS AND METHODS

CRUDE LENS AND LYOPHILISED POWDER

4.1.1 Isolation and preparation of crude lens solution and lyophilised powder

A large number of fresh bovine eyes were procured from a licensed slaughter house and was immediately brought to the laboratory in an ice box. The eyes were dissected within 2-3 h of their arrival. The lenses were separated carefully from the intact eye by removing its surrounding vitreous, aqueous and capsular materials. These were then kept in -20 ^{0}C for future use.

The lenses stored at -20 ^{0}C were thawed and a viscous solution of it was prepared using distilled water. The prepared solution was then kept overnight at around -50 ^{0}C for lyophilization. The lyophilized sample was then weighed and the powder obtained was stored at -20 ^{0}C for further characterizations. The concentrations of the crude lens protein solution and the lyophilized lens powder solution were analyzed by using Bradford assay method [20].

4.1.2 SDS-Poly Acrylamide Gel Electrophoresis

Laemmili's discontinuous buffer system was used for the SDS-PAGE analysis of the crude lens solution and the lyophilized powder solution [21]. Electrophoresis setup, that is, a GeNei vertical mini gel system (Merck specialities Pvt. Ltd) was used according to the instructions given by the manufacturer. Electrophoresis was done using 12% polyacrylamide separating gels and 5% stacking gels at a constant voltage of 90 volts in the presence of 10% SDS (Loba Chemie Pvt. Ltd., Mumbai, India) and were stained with Coomassie Brillliant Blue R 250 (Sisco Research Laboratories Pvt. Ltd., Mumbai, India). Samples were boiled in loading buffer (Tris-HCl, pH=6.8; 2 % SDS, reducing agent DTT (HiMedia), β-mercaptoethanol (0.5 ml), sinking agent glycerol and a marker dye Bromophenol blue) for 5 min. prior to electrophoresis and up to 10-30 µl of it was added in each well.

4.1.3 FTIR Spectroscopic study:

Fourier transform infrared (FTIR) absorption spectra of the crude lens solution and the lyophilized powder solution prepared in distilled water at same concentration (approximately 10mg/ml) was analyzed using a FTIR spectrometer (Alpha- E, Bruker, Germany), attached with a ZnSe ATR cell. The analysis was done at a wavenumber range of 4000 cm^{-1} – 500 cm^{-1}. For each sample, a total of 25 scans at 8 cm^{-1} resolution was used. The spectra were obtained by subtracting the portion corresponding to distilled water.

It is known that the shape of the amide I band of globular proteins is characteristics of their secondary structure [22]. Therefore, in order to analyze the secondary structure of the proteins, deconvolution of the amide I band (~1600-1700 cm^{-1}) contours were performed. This was followed by second order derivatization and Gaussian curve fitting.

4.1.4 Circular Dichroism study

Far-UV CD measurements of the crude lens solution (1mg/ml) and the lyophilized lens protein powder solution (1mg/ml) prepared in distilled water was carried out using Jasco J-1500 CD Spectrometer (Jasco, Tokyo, Japan). The solutions were scanned from 250 nm to 190 nm in a quartz cuvette having 1 mm pathway length. The scan was done at a scan rate of 10 nm min^{-1} using a bandwidth of 1 nm and a response time of 2 s. Each spectrum obtained was an average of three scans, and a reference scan of the corresponding buffer (here distilled water) was subtracted. The temperature (30 ^{0}C-90 ^{0}C) of the sample was controlled using a Peltier element, and it was increased at a rate of 3 ^{0}C min^{-1} in between the measurements [23]. The resultant spectra were expressed in units of molar ellipticity (deg. cm^2 $dmol^{-1}$) by using the following equation:

$$[\theta]_{mrw,\lambda} = \left((MRW * \theta_\lambda) / 10 * d * c \right)$$

where, MRW= mean residual weight of the lens protein crystallin, θ_λ= ellipticity in degrees, d=optical path length in cm and c= concentration of protein in g/l.

4.1.5 ANS fluorescence study

The accessibility of the hydrophobic surfaces of the crude lens solution and the lyophilized lens powder solution was probed using ANS (8-anilinonaphthalene-1-sulphonic acid, Sigma) fluorescence studies. A stock solution of ANS (4mM) was prepared and this was then diluted using

10 mM phosphate buffer, pH=7.0. A fluorescence spectrometer (PerkinElmer LS 55) was used to record the spectra in a 1 cm path length cuvette. Excitation wavelength of 390 nm (band pass 5 nm) was used and the emission spectra were recorded between 400 nm and 600 nm (band pass 10 nm) at a scan rate of 100 nm min^{-1}. Solutions of ANS (50 µM) in buffer and ANS (50 µM)/protein (50µg/ml) were prepared in duplicates and were incubated for 5-10 min. before recording the spectra. The spectra obtained from these solutions were subtracted with the spectrum of the buffer only, which was taken as a blank.

4.1.6 Chaperone Assay

The chaperone activity of the lyophilized lens powder was performed by measuring the reduction of disulfide bonds in insulin as described previously [24] [25]. In brief, insulin (0.4mg/ml,) was dissolved in 0.05 M sodium phosphate buffer containing 0.15 M NaCl (pH 7.2) and the reaction was initialized by the addition of 25 µl of 1M DTT in the absence or presence of the lyophilized lens powder in different w/w ratios to insulin (0.16:1, 0.4:1). The assays were carried out at 37 ^{0}C in a Cary-100 UV/vis spectrophotometer (Agilent Technologies, India) and the light scattering was continuously monitored at 360 nm for up to 60 min. All the assays were performed in duplicates. The chaperone activity was calculated using the following equation:

$$Chaperone\ activity = 1 - \frac{A_{\infty}}{A_{\infty,control}}$$

ELECTROSPINNING OF THE CRUDE LENS POWDER

4.1.7 Solution Preparation for Electrospinning

The lyophilized lens protein powder at different concentrations (5%, 10%, 15%, 20%, 30%, 40%) were dissolved in trifluoroacetic acid (TFA- 99%, HiMedia) in small glass bottles and were mixed on a magnetic stirrer in order to achieve homogenous solutions. The proteins were mixed in different concentrations to achieve different viscosity. These solutions were then taken for electrospinning.

4.1.8 Electrospinning

The prepared lyophilized lens protein solution at different concentrations with TFA were electrospinned by a nozzle-free method. In this method, a drop of the prepared solution was placed on the sample holder and the obtained fibers were collected on the aluminium foil that is pasted at the top where the collector is present. The whole setup is enclosed in a closed vacuum chamber which is provided with a high voltage power supply. Electrospinning of the solutions of lens protein and TFA were carried out with a high voltage power supply set at 30-40 kV with an air gap distance of 12 cm. The experiments were performed at room temperature and the samples were kept in a desiccator for overnight.

4.1.9 Scanning Electron Microscopy

The morphology of the prepared lens protein nanofibers were analyzed by using a Field Emission Scanning Electron Microscope at an accelerating voltage of 10-15 kV. Fiber samples were cut from different locations on the electrospun mat and were mounted onto stubs for sputter coating by gold using (QS 1050 Quorum Tech.) sputtering before scanning with (Nova Nano Sem, FEI). Fiber diameter of the electrospun nanofibers were measured from the obtained micrographs using ImageJ software developed at National Institute of Health, USA. For each sample, at least five scanning electron micrographs were captured from different spots.

4.1.10 X-Ray Diffraction study

X-Ray Diffraction (XRD) analysis of the lyophilized lens protein powder and the electrospinned fiber was conducted using a Rigaku, Ultima IV Multipurpose XRD Diffractometer (Rigaku Co., Tokyo, Japan) having a Cu-Kα radiation source and operated at 40 kV, 40 mA. The analysis was done in the 2θ range of 3^0-50^0 at a scan rate of 3^0 min^{-1}.

4.1.11 FTIR Spectroscopic study

The Fourier transform infrared (FTIR) absorption spectra of the electrospinned nanofibers were obtained similarly as mentioned above. The obtained spectra was deconvoluted followed by derivatization and Gaussian curve fitting in order to analyze the changes in the secondary structure of the lyophilized lens protein after electrospinning.

4.1.12 Solubility study

The solubility study of the electrospinned nanofibers were performed in distilled water in order to check its solubility and thus the concentrations of the protein was measured at different time intervals. In brief, a 2mg/ml solution of the electrospinned fibers was made. These were then mixed properly and centrifuged at 13,400 rpm for 10 min. After centrifugation aliquots were prepared by taking 50 µl of each sample. This process of mixing and centrifuging was repeated at regular time intervals and thus the aliquots collected were measured for its protein concentration using Bradford assay method [20]. All the measurements were performed in duplicates.

4.1.13 *In vitro* studies

4.1.13.1 Cytotoxicity and cell proliferation studies

In vitro cytotoxicity and cell proliferation studies of the lyophilized lens powder and the electrospin fibers were performed using Adipose derived stem cells (ADSCs, HiMedia Pvt. Ltd., Mumbai, India). The cells were maintained in Dulbecco's Modified Eagle Medium (DMEM) supplemented with 10 % Fetal Bovine Serum (FBS) and 1% antibiotics mixture (penicillin/streptomycin) at 37 °C (5% CO_2 and 95% humidity). In brief, after cells reached 80% confluence, they were harvested using 0.05% trypsin/EDTA solution and thus were subsequently seeded at a cell concentration of $1x10^4$ cells/ml onto the 96 well plates. These were incubated for 24 h and after properly evaluating the adherency of the cells the sterilized samples (100 µg/well) were added into the wells. For sterilization, the samples (1mg/ml) were dissolved in PBS and mixed and centrifuged properly in order to get a homogenous solution. This solution was then filter sterilized using a microfilter (0.22 µm). The plate was maintained for 7 days and thus the metabolic activity of cells was monitored using MTT assay after every 2, 5, and 7 days. All the assays were done in triplicates.

4.1.13.2 Confocal Microscopy

The confocal microscopic study of the elctrospun fibers were done in order to see the spreadibility as well as the attachment of the cells onto the fibers. This study was also conducted to see how the cytoskeletal structures of the cells are changing in the presence of the fibers in compared to the control samples. For the study, first the electrospun fibers were sterilized in UV for 30 min., followed by keeping in 70% ethanol solution for 30 min. and then finally the fibers were washed thoroughly with PBS for three times. This whole process was done after placing the fibers on the cover slip. After this the Adipose derived stem cells were seeded onto these fibers at a cell concentration of $0.5x10^4$ cells/sample and these were then allowed to adhere onto the fibers for some time. The complete media (DMEM, 10% FBS and 1% antibiotics) were then added onto the samples without much disturbing the cells. This was then kept for 24 h incubation at 37 ºC in a CO_2 incubator maintained at 5% CO_2 level and 95% humidity. After 24 h of incubation, the fixation of the cells onto the fibers were done by decanting the media and adding 4% paraformaldehyde for 10-15 min. This was then washed thoroughly with PBS for approximately three times. Then the process of permeabilization was carried on for 15 min. by using permeabilization buffer (0.25% Triton-X 100 in PBS) followed by a through PBS wash for three times. Washing with PBS after each step was a must and was the most important step. Then the blocking buffer (2% BSA in PBS) was used for 45 min. to block the things. Then a final wash with PBS for three times was done. After this, in order to view the cytoskeletal structures of the cells, that is, the F-actin present in the cytoskeleton of the cells as well as the nucleus of the cells, the prepared samples were stained with TRITC phalloidin red for 7-8 min. and DAPI for 2 min. respectively. After each staining a thorough PBS wash was done for three times, keeping PBS for

at least 5 min. in each wash. The prepared samples were then viewed under Leica TCS 128 confocal microscope.

4.1.13.3 Cell attachment study using Scanning Electron Microscope

Cell attachment studies on the fibers in compared to the control samples were also done using Field emission scanning electron microscope (Nova Nano Sem, FEI). In brief, for this study the fibers samples were first sterilized in the same way as they were sterilized for the confocal microscopy as well as the cytocompatibility studies. The samples for this analysis were prepared in very small glass slides. After sterilization process the ADSCs were seeded in the same concentration as used for the confocal microscope and then were kept in a CO_2 incubator for 24 h. After 24 h, the complete media which was supplemented for inducing cell attachment and growth was decanted and this was then washed thoroughly with SEM buffer. Then the fixation of the cells onto the fibers were done using SEM grade glutaraldehyde (25% was made to 2.5% using SEM buffer) and this was kept for. After this serial dehydration of the samples were done using ethanol gradient (30%, 40%, 50%, 60%, 70%, 90%, 100%)

4.1.14 Statistical Analysis

The experiments were performed in triplicates and all the results obtained were mentioned as an average ± S.D. Statistical analysis of the obtained data was done using unpaired t-test and one-way ANOVA through IBM SPSS Statistics 20.0. The results having p value of ≤ 0.05 were considered to be the statistically significant results.

4.2 RESULT AND DISCUSSIONS:

CRUDE LENS AND THE LYOPHILIZED POWDER

4.2.1 Preparation of lens solutions and SDS-PAGE:

The crude lens solution was prepared in a sterile manner. The lenses were washed properly with normal saline and the capsules enclosing the lens were removed before being used for solution preparation. The lenses were then dissolved in cold distilled water, in lens to distill water ratio of 1:4 for around 1 h. This solution was then lyophilized to prepare the lens protein powder. Further physical characterizations of the crude lens solution and the lyophilised powder were carried out using different studies. The concentration of the crude lens solution and the lyophilized powder solution (prepared 1 mg/ml in distilled water) was measured using Bradford assay method. The concentrations were found to be 6.5 mg/ml and 0.978 mg/ml respectively.

SDS- PAGE of the crude lens solution and the lyophilized powder was carried out in order to confirm the presence of the bands corresponding to the major lens protein crystallins. Fig. 4.1 shows the SDS-PAGE of both the samples along with the medium range and broad range markers in lane 1 and 4 marked as marker 1 and marker 2 respectively.

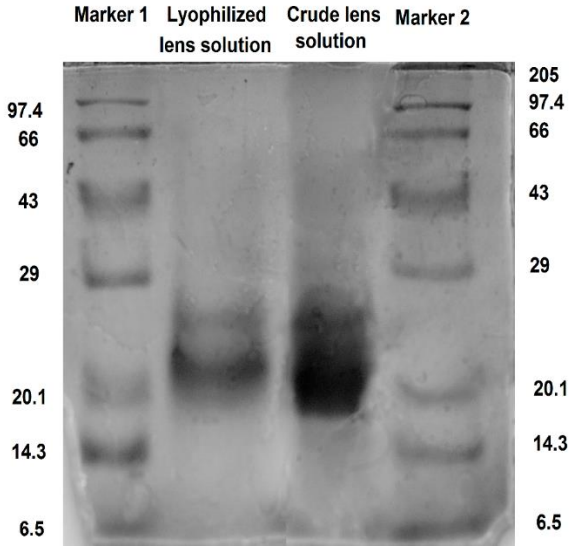

Figure 4.1 SDS-PAGE of the lyophilized lens powder and the crude lns solution

4.2.2 FTIR Spectroscopic studies:

The conformation of the prepared protein solutions were analyzed using ATR-FTIR spectrometer. The absorption spectrum of the crude lens solution and the lyophilized lens protein powder solution in distilled water along with the characteristic bands of protein, is represented in Fig. 4.2 and Table 4.1 respectively. The portions in the spectra corresponding to the distilled water were subtracted from the final spectrum.

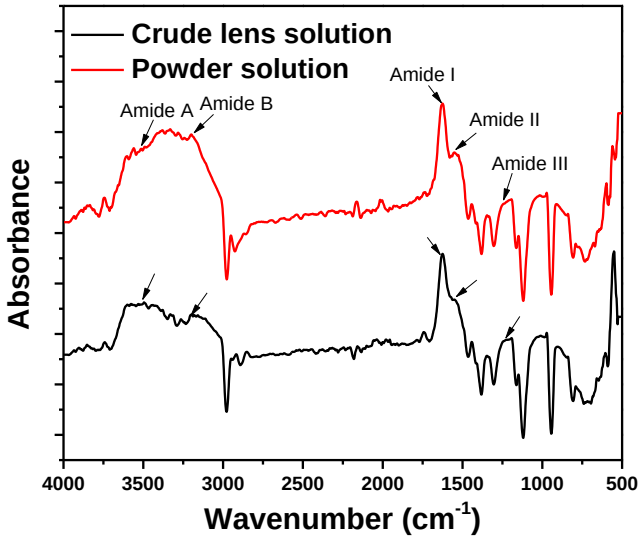

Figure 4.2 ATR-FTIR graph of the bovine lens protein solution before and after lyophilisation

There are 9 characteristic bands (namely amide A, B, I, II, III … VII) that are found in the structural repeat units of proteins or peptide groups. The Fermi resonance between the amide II band and the N-H stretching vibration give rise to amide A and amide B band at around 3500 cm^{-1} and 3100 cm^{-1} respectively. The two major bands of the protein infrared spectrum are the amide I band (1600-1700 cm^{-1}) and amide II band (1510-1580 cm^{-1}). Amide I band is mainly associated with the stretching vibrations of the C=O (70-85%) and C-N groups (10-20%) and is directly related to the backbone conformation and the hydrogen bonding pattern of proteins. The N-H bending vibration (40-60%) and the C-N stretching vibrations (18-40%) results in the amide II band formation [26]. Amide III band (1240 cm^{-1}) corresponds to C-N stretching vibrations and N-H bending vibrations. Among the different protein absorbance peaks shown, the amide I band

contour of both the crude lens and the lyophilized powder solutions at room temperature showed a maximum at 1632 ± 2 cm^{-1}. This is a characteristic feature of proteins having a high proportion of β-sheet secondary structure. To further confirm this qualitative analysis, deconvolution using second-order derivative method and band fitting of the amide I band spectra of the lens proteins both before and after lyophilization were done. [27] [28]

Table 4.1 Major protein infrared frequencies and confirmations of the bovine lens protein

Bovine lens protein	**Infrared frequencies (cm^{-1})**			**Major Backbone Confirmation**
	Amide I	Amide II	Amide III	
Crude lens solution	1631	1549	1240	β-sheet
Lyophilized powder solution	1633	1550	1243	β-sheet

The deconvoluted and curve fitting spectrum of the lens proteins both before and after lyophilization revealed the presence of at least five bands in the amide I region (Fig. 4.3). The peaks around 1635, 1632, 1619, 1616 cm^{-1} can be assigned to β-sheet components, and are in good agreement with the previous infrared studies [22] [29] [30] [31] [32] [33] [34]. The weaker bands at around 1651-1653 and 1665 cm^{-1} are usually assigned to α-helices and turns, respectively [22] [35] [27]. The bands around 1605-1611 cm^{-1} represents side chain vibrations of tyrosine and/or arginine [36] [37].

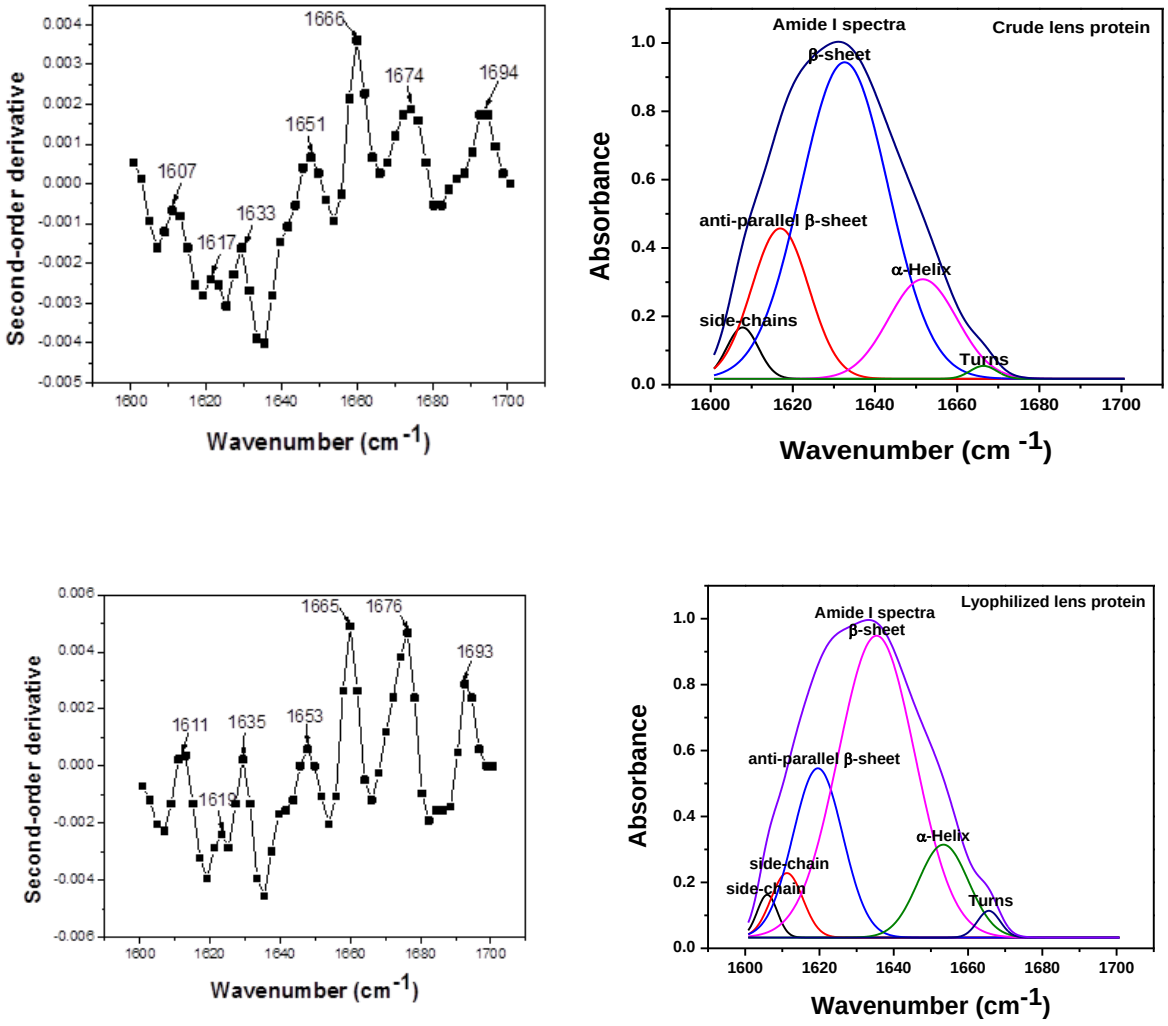

Figure 4.3 Second-order derivative and curve fitting spectrum of Crude lens protein and lyophilized lens powder solutions

Quantitative band fitting analysis of crude bovine lens and the lyophilized powder solutions (Table 4.2) shows that the fractional area of the parallel (∥) β-sheets are 63 and 61 %, respectively, whereas, the anti-parallel (anti-∥) β-sheet content is found to be 22 and 27 % respectively. The result shows that though there is minute difference in the ∥ β-sheets content of the two sample, a significant difference can be seen in the anti-∥ β-sheets content. The value of the α-helical band 1651-1653 cm^{-1} were found to be same (18%) in both the crude and the lyophilized lens powder solution, thereby denoting that the α-helical structure of the lens proteins after lyophilization is

unchanged. The content of the turns and the side-chains were found to be more in the lyophilized lens powder solutions in compared to the crude lens solution. Thus it can be said that the lyophilization affects the secondary structure of the proteins though not significantly but minutely. Hence, it can be said that after lyophilization the randomness of the protein increases.

Table 4.2 Deconvoluted curve assignments, infrared frequencies and the secondary structure estimates of the bovine lens protein

Bovine Lens Protein	Deconvoluted curve assignments	Infrared frequencies (cm^{-1})	Secondary structure estimate (%)
Crude lens solution	β-sheets (∥* and anti-∥)	1632 (∥), 1616 (anti-∥)	63 (∥), 22 (anti-∥)
	Helix	1651	18
	Turns	1666	4-5
	Side-chains	1607	7
Lyophilized lens solution	β-sheets (∥ and anti-∥)	1635 (∥), 1619 (anti-∥)	61(∥), 27 (anti-∥)
	Helix	1653	18
	Turns	1665	8-9
	Side-chains	1605, 1611	9-12

*∥ indicates parallel β-sheets

4.2.3 Circular Dichroism studies:

Fig. 4.4 shows the CD spectra of the crude lens solution and the lyophilized powder solution prepared at 1mg/ml concentration at increasing temperature (30-90 ⁰ C). The spectrums were studied to quantitatively estimate the secondary structure as well as the stability of the crude proteins before and after lyophilization [23] [38]

The CD spectra of the crude lens solution represented below show a negative band in between 210-220 nm and a positive band between 195-205 nm at almost all temperatures, which is a characteristic of an all β-sheet protein [39] [40]. Spectra of the β-sheet proteins are found to be diverse in nature in compared to the α-helical proteins because β-sheets may be present in different confirmations, such as, parallel, anti-parallel or mixed and it can be twisted in many ways. As we vary the temperature from 30-90 °C, no significant variation was found in the spectra of crude lens

solution, though a slight shift in the spectra towards higher wavelength was seen from temperature ~60-70 ° C onwards.

Similarly, the CD spectra of the lyophilized lens protein solutions at varying temperature has been represented below. The spectrums from temperature 30-50 °C showed similar trend like the crude lens protein solution thereby, showing the abundance of β-sheet proteins. The variation in the spectrum for the lyophilized sample starts at temperature 60 °C showing changes in the secondary structure of the proteins in these sample. There is a shift in the negative band towards lower wavelength and the spectra at temperature 90 °C shows the maximum of the negative band at around ~203 nm thereby showing more disordered (random coil) structures.

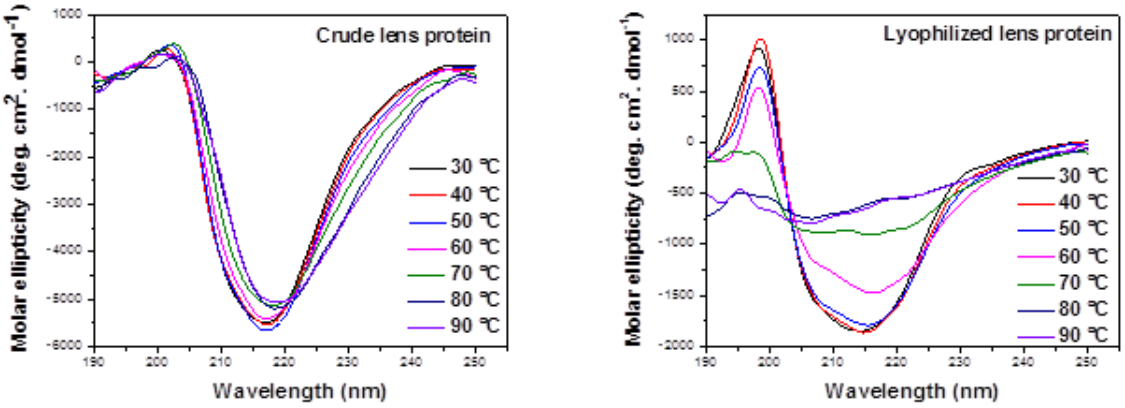

Figure 4.4 CD spectra at different temperatures of Crude lens protein and Lyophilised lens protein

The percentage of different secondary structures observed in the crude lens solution and the lyophilized lens solution has been shown in Table 4.3.

Table 4.3 CD analysis using CONTIN and K2d programs

Secondary structures	**30 ^{o}C**		**40 ^{o}C**		**50 ^{o}C**		**60 ^{o}C**		**70 ^{o}C**		**80 ^{o}C**		**90 ^{o}C**	
	Crude	**Lyo**	**Crude**	**Lyo**	**Crude**	**Lyo**	**Crude**	**Lyo**	**Crude**	**Lyo**	**Crude**	**Lyo**	**Crude**	**Lyo**
α-Helix	**2.6**	**2.6**	**2.6**	**2.6**	**2.6**	**2.6**	**2.6**	**2.7**	**2.6**	**2.6**	**2.7**	**2.6**	**2.7**	**2.7**
β-sheets	**40.3**	**40.6**	**40.2**	**41.1**	**40.2**	**40.6**	**40**	**41**	**40.2**	**40.7**	**40.2**	**40.8**	**39.8**	**40.8**
Turns	**19.4**	**19.3**	**19.4**	**19.5**	**19.4**	**19.3**	**19.4**	**19.5**	**19.3**	**19.3**	**19.1**	**19.4**	**19**	**19.4**
Random	**37.7**	**37.5**	**37.8**	**36.8**	**37.9**	**37.4**	**37.9**	**36.8**	**37.9**	**37.4**	**38**	**37.2**	**38.5**	**37.1**

Secondary structures	**30 ^{o}C**		**40 ^{o}C**		**50 ^{o}C**		**60 ^{o}C**		**70 ^{o}C**		**80 ^{o}C**		**90 ^{o}C**	
	Crude	Lyo	Crude	Lyo	Crude	Lyo	Crude	Lyo	Crude	Lyo	Crude	Lyo	Crude	Lyo
α-Helix	4	7	4	7	4	7	4	7	4	5	4	5	4	5
β-sheets	48	45	48	45	48	45	48	46	48	47	48	47	48	47
Random	48	48	48	48	48	48	48	48	48	48	48	48	48	48

The analysis of the obtained spectrums were done using the CONTIN and the K2d programs that are available from the online web-server DICHROWEB. The CONTIN program gives the estimation of α-helix, β-sheets, turns and random structures, whereas, the K2d program gives the estimation of only α-helix, β-sheets and random structures.

4.2.4 ANS Fluorescence studies:

The changes in exposed hydrophobic surface of the crude lens protein and the lyophilized powder solution was monitored by probing with ANS fluorescence. Fig. 5 shows the fluorescence spectra of only ANS, ANS with the crude lens protein, and ANS with the lyophilized lens powder. It is a

known fact that ANS have a very low fluorescence yield in aqueous environment which increases significantly when it binds to a hydrophobic environment. The fluorescence of ANS is found to be at around 530 nm. In the presence of crude lens solution, its fluorescence was found to be blue-shifted and the maximum emission spectra was ~470 nm. Also the emission intensity increases, indicating the increased availability of hydrophobic surfaces on the crude lens solution. [41]

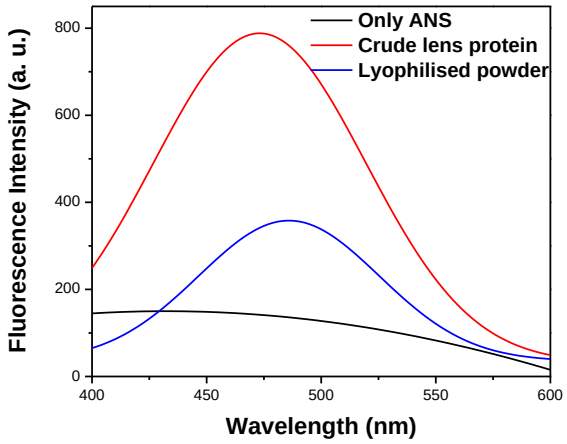

Figure 4.5 Fluorescence spectra of ANS (black), in the presence of crude lens protein (red) and in the presence of lyophilized powder (blue)

On the other hand, the maximum emission spectra for the lyophilized lens powder solution was ~490 nm, and its emission intensity was found to get decreased in compared to the crude lens solution. The surface hydrophobicity of the lyophilized lens powder solution was nearly half that of the crude lens solution indicating that certain structural changes are happening in case of the lyophilized lens powder solution which causes less exposure of its hydrophobic surfaces in compared to the crude lens solution. The p values obtained were ≤ 0.05, thus we can say that the datas collected were found to statistically significant.

4.2.5 Chaperone activity studies:

The chaperone activity of the lyophilized lens protein was evaluated using insulin as a client protein. This study was performed in order to observe that, whether the lyophilized lens protein can retain its chaperone activity after lyophilization. Aggregation measurements of insulin was carried out in the presence of DTT at 37 ° C. Fig. 6 represents the chaperone activity studies of the insulin alone as well as in the presence of the lyophilized lens protein at two different concentrations.

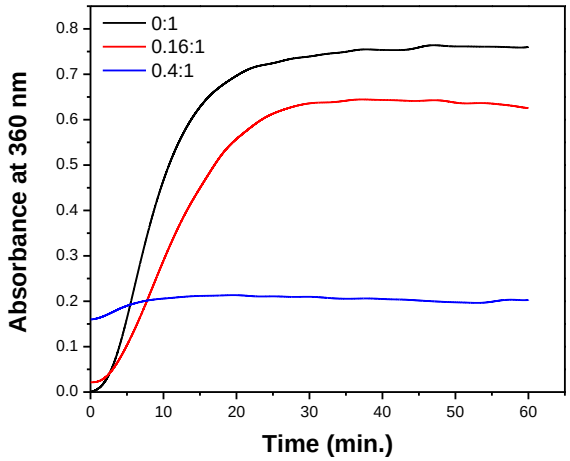

Figure 4.6 Chaperone activity studies using insulin in the absence or presence of the lyophilized lens protein

The lyophilized lens proteins were found to be effective at suppressing the aggregation of insulin at both the concentrations. At a 0.16:1 (w/w) ratio of lyophilized lens protein to insulin, the aggregation of insulin was suppressed by only 18%, but when the ratio of lyophilized lens protein to insulin was increased to 0.4:1 (w/w), the aggregation was suppressed by 76%. Thus the results show that the lyophilized lens protein retain its chaperone functionality and thus prevent aggregation of the insulin proteins at physiological temperature. The results were shown be statistically significant and the p values were found to be ≤ 0.05.

ELECTROSPINNING OF THE CRUDE LENS POWDER

4.2.6 Preparation of Electrospinning solutions

The lyophilized lens protein powder were mixed with 99% TFA in different increasing concentrations, that is, 5%, 10%, 15%, 20%, 30%, and 40%. The proteins were mixed in such concentrations in order to achieve solutions having varying viscosities. These solutions were prepared in glass bottles and were thoroughly mixed in a magnetic stirrer in order to achieve a homogenous solution. The prepared solutions were then electrospinned using the nozzle-free electrospinning machine Nanospider. In this way the process of electrospinning was optimized and it was found that from 10% protein solution onwards very thin fibers were formed. The fibers formed were so thin that it was hardly visible from the naked eye. At protein solution of concentration 40% very fine fibers were formed. The video showing the electrospinning machine forming the fibers has been provided in the supplementary data (Supplementary video, S1). All the fibers were formed at a voltage of around 30 kV with a distance of 12 cm between the sample holder and the collector. The fibers formed were collected in an aluminum foil and their morphology was observed using the Field Emission Scanning Electron Microscope (FESEM) and thus the size of the fibers were analyzed.

4.2.7 Scanning Electron Microscopy

The morphology of the electrospun lens protein fibers was assessed using Field Emission Scanning Electron Microscope (FESEM) and the size of the fibers was analyzed using the Image J software. Fig. 7 a-f shows the SEM micrographs of the protein/TFA solutions made in different concentrations, 5-40%. From the micrographs, it is evident that a proper smooth fibers without any

bead defect was formed only with the highest protein concentration solution that is 40%. From Fig. 7a-e, shows the micrographs having only beads or having beads with little amount of fibers.

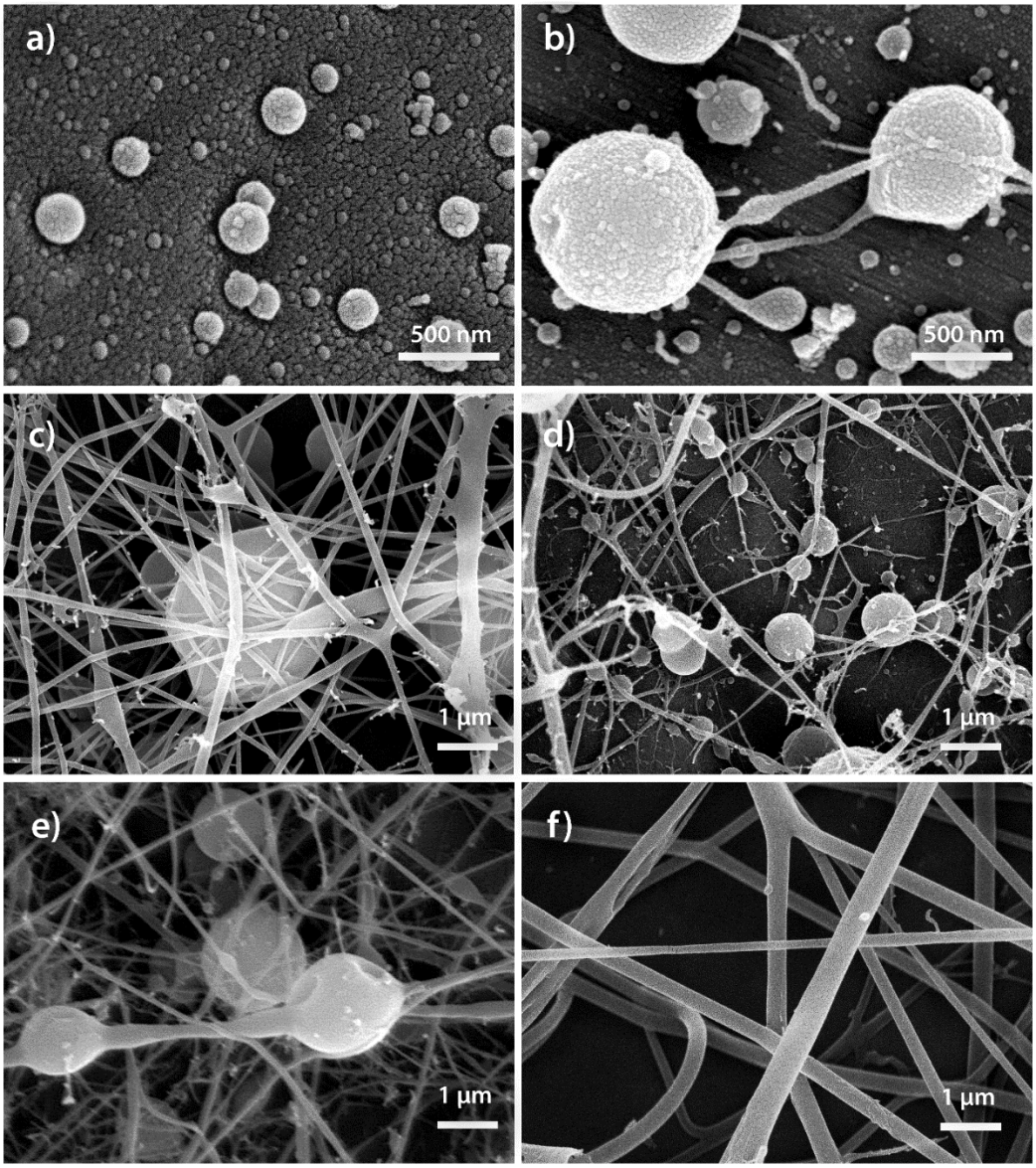

Figure 4.7 SEM micrographs of the electrospun lens protein/TFA at different concentrations, a) 5%, b)10%, c)15%, d)20%, e)30% and f)40%

These micrographs represents the protein concentration solution from 5-30%. It was observed that the solution containing lowest concentration of protein that is 5% formed only beads, whereas, there were few fibers seen coming out in the solution containing 10% protein. The micrograph of

the 15 % protein/TFA solution, Fig. 7c showed more number of fibers and less number of beads in compared to the 10% protein solution. Thus as we observe the micrographs of higher protein content solutions (20% and 30%) we find that the formation of the fibers are more in compared to the beads. Finally, in the micrographs of the 40% protein solution only smooth fibers of the lens protein was observed and the size of the fibers was found to be in the nanometer range. The average size of the nanofibers was found to be around ~216.4 ± 3.1 nm.

4.2.8 X-Ray Diffraction studies

The X-Ray diffraction studies of the lyophilized lens powder and the electrsopun fibers were done in order to see if there is any phase change or extra phases present after electrospinning in compared to the lyophilized lens powder. The XRD profiles of both the powder and the fibers have been shown in Fig. 4.8. The lens crystallin lyophilized powder showed a small peak at about 9.5^0 (2θ) and a narrow peak at around 20.5^0 (2θ) corresponding to the β-sheet structure. [42]. Thus proving that the lens proteins are β-sheet rich proteins. On the other hand, the XRD profile of the electrospun fibers showed a narrower and a small peak at 9.5^0 (2θ). The peak at around 25^0 (2θ) was also observed in case of the fibers.

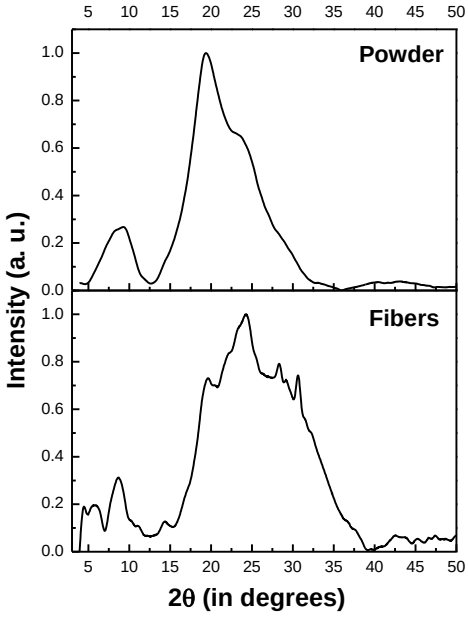

Figure 4.8 XRD spectra of the lyophilized lens powder and the electrospun fibers

Other interesting thing to observe in the XRD profile of the fibers is that there were many small peaks observed here and there in compared to the powder fibers. This shows that there is definitely some changes happening in the electrospun fibers in compared to the lyophilized powder samples. A distinct peak at around 4.5° (2θ) shows that the fibers are showing amyloid like characteristics. Also a peak at around 14.7° (2θ) corresponds to peak showing amyloid fiber like characteristics. These characteristics are specifically seen due to the cross-β structure formations by the amyloids due to the intramolecular hydrogen bonding [43]**.** Hence, may be these fibers that were electrospun are showing these characteristics and turning into amyloids.

4.2.9 FTIR Spectroscopic studies

The FTIR spectroscopic study of the electrospun fibers was done and was compared to the lyophilized lens powder in order to see if there is any major structural changes happening between the lyophilized lens powder and the electrospun fibers that were prepared by mixing with TFA. The FTIR spectra of the electropsun fibers are shown in Fig. 4.9. The spectra shows all the basic peaks that are present in a protein.

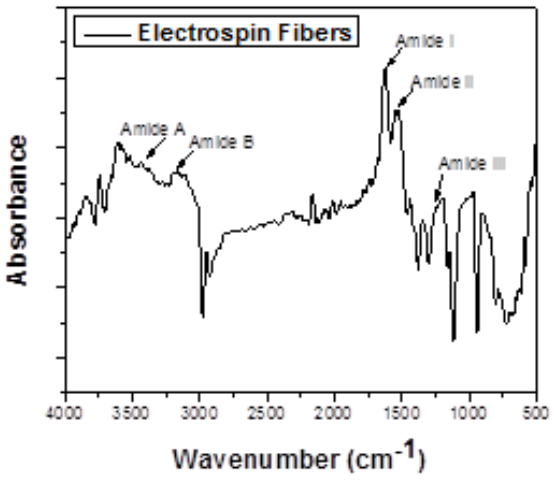

Figure 4.9 FTIR graph of the electrospun fibers

The amide I spectra of these fibers was then deconvoluted and curve fitted similarly as mentioned previously in order to estimate the secondary structural content of the electrospun fibers as well as to see the distinct different peaks that were observed in the fibers in compared to the lyophilized powder. The second-order derivative graph showing the total number of peaks found in the amide 1 spectra as well as the curve-fitted graph are shown in Fig. 4.10.

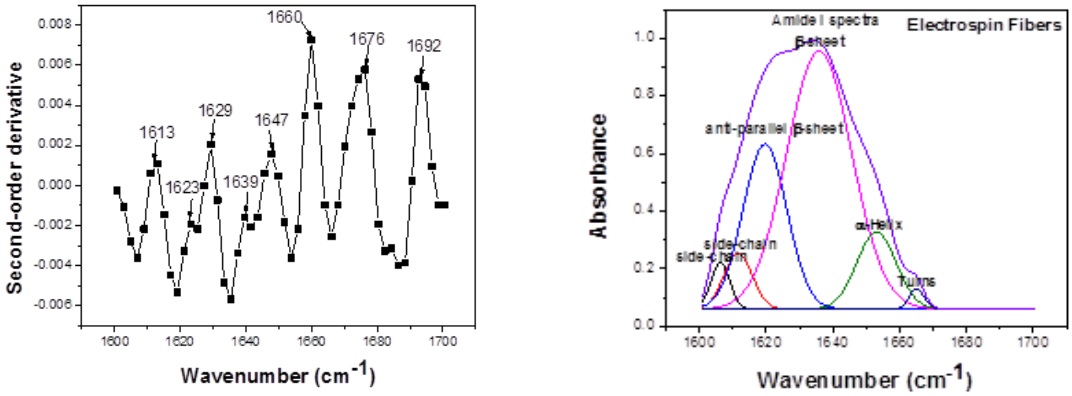

Figure 4.10 Second-order derivative and curve fitted FTIR spectra of the electrospun fibers

The deconvoluted spectra of the electrospun fibers showed two distinct peaks in the wavenumber range of 1620-1640 cm^{-1} in compared to just one peak shown by the lyophilized powder in that range. The peaks present in this range corresponds to the anti-parallel β-sheets structure as previously mentioned. An increase in the number of bands of the anti-parallel β-sheets is also an indication that the fibers are showing amyloid like characteristics. This is because the amyloid fibers have a tendency to increase the number of anti-parallel β-sheets band by splitting them into one or more bands. Also, after the curve fitting was done there was no significant changes seen in the electrsopun fibers in compared to the lyophilized lens protein. Hence, we can say that no major changes as such is happening in the fibers after the electrospinning process. Although, the amyloid like characteristics that this electropsun fiber shows need to be confirmed by doing further studies.

4.2.10 Solubility studies

The solubility studies of the electrospun fiber was done in order to check whether the fibers are getting solubilized or not. This was done in distilled water for around 24 h. The non-solubility of the fibers in distilled water also indicated that may be these fibers are turning into amyloids as

amyloids are also the fibrous proteins that are insoluble. The test was carried on for 24 h and at different time intervals 50 µl aliquots were collected and the protein concentration was measured using Bradford assay method. Initially 2 mg/ ml solution of fiber in distilled water was prepared. After analyzing the protein concentration for 24 h, it was seen that only 380 µg of the proteins got solubilized from the 2mg fibers that were taken initially. This proved that the solubility of the fibers in distilled water was negligible thus proving that the fibers prepared are insoluble fibers.

4.2.11 *In vitro* studies

4.2.11.1 Cytocompatibility and cell proliferation studies

The cytocompatibility and the cell proliferation studies of the lyophilized lens powder as well as the electrospun fibers were done in order to see the biocompatible nature of the lens proteins crystallin. Fig. 4.11 shows the biocompatibility studies of the lyophilized lens powder and the electrospun fibers for 7 consecutive days using MTT assay method. 100 µg of both the lyophilized lens powder as well as the elctrospun fibers were added into a 96 well plates that were pre-seeded with Adipose derived stem cells. The study was carried on for 7 consecutive days by taking MTT readings for every 2, 5 and 7 days. It was observed that there was a significant increase in biocompatibility of the lyophilized lens powder in compared to the controls that were prepared for all the three days for which the cell cytotoxicity studies were done. On the other hand, the electropsun fibers did not show that much significant increase in its biocompatibility compared to the control samples. Also it was seen that the proliferation of the cells on the electrospun fibers were less in compared to the lyophilized powder as well as to the control. Although the cytocompatibility as well as the cell proliferation was less in the electrospun fibers, still the cells growth was maintained and they were found to remain healthy in presence of these fibers for 7 consecutive days. Therefore, we can conclude that though these fibers are showing less

compatibility with the cells in compared to the lyophilized powder still overall its showing biocompatible nature. One more thing is to be noted that the lyophilized lens powder got electrospun by mixing it with pure TFA solution, may be the presence of TFA in the electrospun fiber is causing its reduction in the biocompatibility in compared to the lyophilized powder.

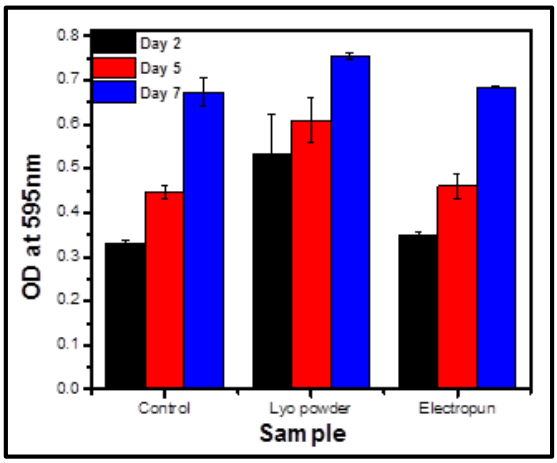

Figure 4.11 Cytocompatiblity studies of lyophilized powder and the electrospun fibers

4.2.11.2 Confocal Microscopy

The confocal microscopic study was done to analyze the morphology of the cells in the presence of electrospun fibers. Fig. 4.12 shows the confocal microscopic images of the elctrospun fibers as well as the control samples. The cytoskeletal structure of the cells was observed by staining the samples with TRITC phalloidin red for viewing the F-actin and the nucleus of the cells were stained with DAPI. This study showed that there are less cells attached on the elctrospun fibers in compared to the control samples. From this study it was seen that in presence of the fibers the cells didn't die, though the cells are showing some changes in the morphology. The presence of less

number of cells attached on the electropsun fibers in compared to the control samples are in accordance with the results obtained from the MTT study.

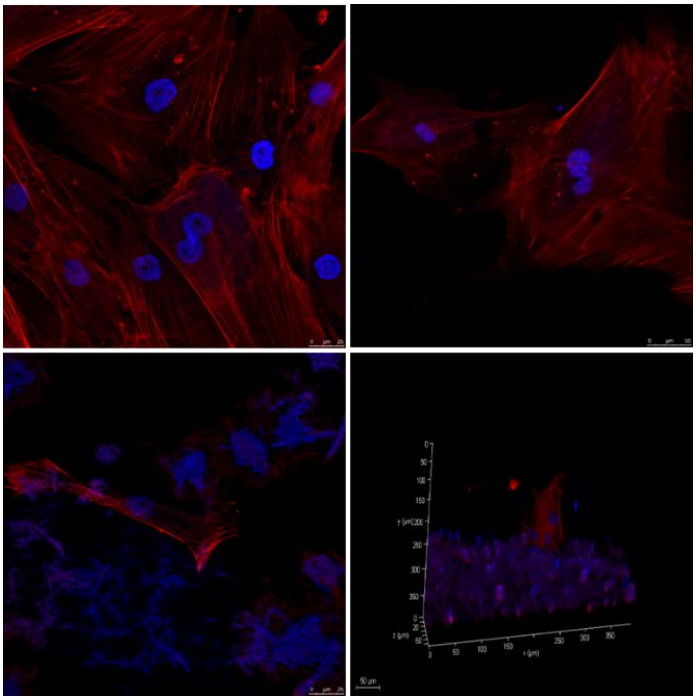

Figure 4.12 Confocal images of the control samples as well as the electrospun fibers

4.2.11.3 Cell Attachment studies using Scanning Electron Microscope

The cell attachment studies using Field emission scanning electron microscope was done to see that whether the cells are attaching at all on the fibers or not. This study was done to better understand the attachment of the cells onto the fibers. Fig. 4.13 shows the SEM micrographs of the cells attached on the control as well as on the electrospun fibers. The micrographs show many cells attached in the control samples, whereas, few cells were seen here and there attached onto the fibers. This study proves that the number of cells that are getting attached onto the fibers are

less but overall the cells are surviving in presence of the fibers. This study also proves that the cells are showing biocompatible nature with the fibers though the adhesion properties of the cells onto the fibers are less. This may be due to the presence of TFA with the help of which these fibers were electrospun.

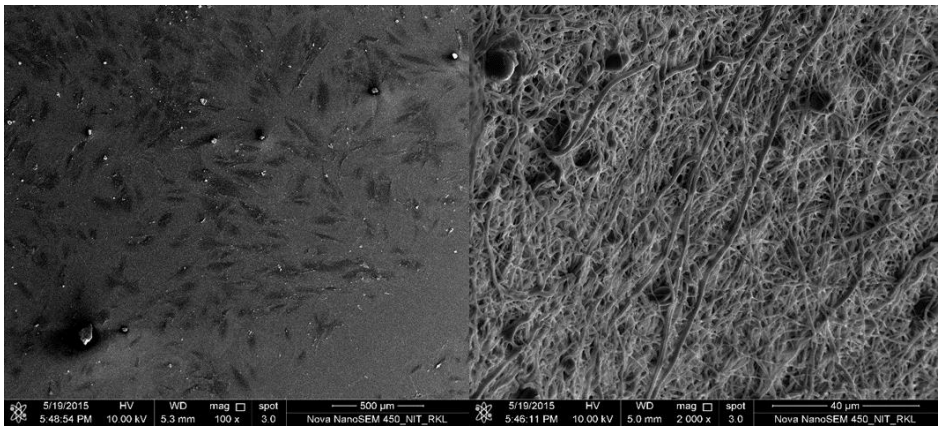

Figure 4.13 SEM micrographs showing cell attachment in the control as well as the electropun fibers

4.3 CONCLUSION

The current study reports the successful comparison of the crude lens solution and the lyophilized lens powder solution on the basis of their structural as well as functional properties and therefore successful preparation of an electrospun fiber from these lyophilized lens powder. The studies showed that there were no significant changes as such, in the structures of the lens powder before and after lyophilization. For this reason, the lyophilized powder was tried to be electrospin using different benign as well as organic solvents and also in the presence of other polymers. Thus the process of electropinning was optimized and finally the intact protein was electrospun using pure TFA solutions. The lyophilized powder and the electrospun fibers were then compared and it was seen that the fibers thus formed are showing amyloid like characteristics. The biocompatibility studies showed that these electrospun fibers are biocompatible in nature and thus possibly can be used for tissue engineering applications in future.

5 SYNTHESIS AND CHARACTERIZATION OF DUAL-ENVIRONMENT RESPONSIVE HYDROGELS

5.1 MATERIALS AND METHODS

HEMA and MC were purchased from HiMedia laboratories Pvt. Ltd. (Mumbai, India). N,N,N,N-tetramethyl ethylenediamine (TEMED) and ammonium persulphate (APS) were procured from Sisco Researh Laboratories Pvt. Ltd. (Mumbai, India) and Rankem (New Delhi, India), respectively. Distilled water was used throughout the study.

5.1.1 Preparation of the MC solutions

A stock solution of 2% (w/v) MC was prepared by dissolving 1 g of MC in 40 ml of water (50 ^{o}C). The final volume was made up to 50 ml using water (50 ^{o}C). The MC solutions were diluted using sufficient amount of water so as to have 1.5 % (w/v), 1.0 % (w/v) and 0.5 % (w/v) MC solutions. All the solutions were incubated at 4 ^{o}C for 30 min.

Thereafter, the solutions were stirred thoroughly in a magnetic stirrer (350 rpm) to obtain homogenous solutions. Freshly prepared MC solutions were used for making the composite hydrogels.

To prepare the hydrogels, HEMA (0.45 g) and MC solutions (1 g) were thoroughly mixed in a magnetic stirrer (100 rpm). Subsequently, 20 % (w/v) APS (0.025 ml) and 40 % (v/v) TEMED (0.025 ml) solutions were sequentially added drop-wise to the homogenous mixture with continuous stirring. The above mixture was incubated for 24h at 37 °C (under nitrogen environment) to allow cross-linking of HEMA. This resulted in the formation of the semi-IPN hydrogels. The compositions of the hydrogels have been tabulated in Table 1. The prepared

hydrogels were stored at 4 ^{o}C for further studies. The sample HM1, which did not contain any MC, was used as the control. The properties of the MC based hydrogel were compared with HM1.

To calculate the percentage conversion of the monomers into insoluble polymer, prepared hydrogels were washed thoroughly in water to remove all the unreacted monomers. They were then dried in vacuum oven at 37 ^{o}C for 2 days. The percentage conversion was then calculated based on the ratio of the total weight of the xerogel after drying and weight of the monomer in the initial mixture.

Table 5.1: Composition of the hydrogels

Sample	Composition of the hydrogels		
	Weight of HEMA (g)	MC Solution	
		Concentration (% w/v)	Weight (g)
HM1	0.45	0.0	1
HM2	0.45	0.5	1
HM3	0.45	1.0	1
HM4	0.45	1.5	1
HM5	0.45	2.0	1

5.1.2 Degree of Polymerization

Fresh hydrogels were prepared as per the above-mentioned procedure in cylindrical shapes (diameter=13.1 mm, height= 17.4 mm). These were then kept at 37 ºC for 24 h to allow cross-linking of HEMA. The prepared hydrogels were used for calculating the average molecular weight of the polymer in between the crosslink points using the Flory- Rehner equation: [44] [45]

$$-[\ln\left(1-v_{2,s}\right)+v_{2,s}+\ \chi_1 v_{2,s}^2]\ =\ \frac{V}{\bar{v}M_c}\left(1-\ \frac{2M_c}{M}\right)\left(v_{2,s}^{\frac{1}{3}}-\frac{v_{2,s}}{2}\right)$$

where $\bar{v}$ the specific volume of the hydrogel, M is the primary molecular mass and M_c is the average molecular mass between cross-links or the network parameters. V is the molar volume of the solvent (water, 18 cm^3/mol), $v_{2,s}$ is the polymer volume fraction in the swollen state determined as roughly the inverse of the equilibrium swelling ratio. χ_1 is the Flory parameter describing the polymer–solvent interaction. [46]

The degree of polymerization (X) was determined as per the equation given below:

$$X=\frac{M}{M_c}$$

5.1.3 Microscopic studies

The microstructure of the hydrogels was visualized under a bright field microscope (LEICA-DM750 equipped with ICC 50-HD camera, Germany). For the analysis, one drop of the reaction mixture was put over a glass slide and covered with a cover slip. The slide was then put in a nitrogen chamber and the reaction was allowed to proceed as per the method described above. The thin films, so formed, were analyzed under the microscope.

5.1.4 XRD studies

The hydrogel were prepared as films for the XRD analysis. Films were converted into xerogels by drying the sample in a vacuum dryer (37 ^{o}C, -0.04 MPa). The XRD analysis was done in the 2θ range of 5-50^{o}. The source of the X-ray was Cu-Kα, which was operated at (40 kV, 40 mA).

5.1.5 FTIR spectroscopic studies

The chemical interactions between the functional groups of the pHEMA and MC were analyzed by FTIR studies. For the study, the hydrogel films were used. The FTIR spectrometer (Alpha-E, Bruker, Germany), attached with a ZnSe ATR cell, was used for the study. The analyses were done in the wavenumber range of 4000 cm-1 -500 cm-1. The original spectra were smoothened and the baseline was corrected using the OPUS software.

5.1.6 Swelling studies

The swelling study of the hydrogels was performed to understand the pH and temperature sensitive nature of the hydrogels. The pH of the swelling media were 1.2 (citrate buffer), 7.0 (phosphate buffer) and 9.0 (phosphate buffer). The studies were conducted at 4 ^{o}C, 25 ^{o}C and 37 ^{o}C. Hydrogels of dimension (diameter=19.5 mm and height= 1.5 mm) were used for the swelling studies. Hydrogels were accurately weighed in a highly sensitive weighing balance (W_i). The hydrogels were put in 12 ml of the swelling media, kept in 6-well plate. Subsequently, the well-plates were incubated at the preset temperature cabinets. At regular intervals of time, the hydrogels were taken out of the swelling media, wiped with Whatman paper and weighed again (W_f). The change in the swelling was noted down. The study was conducted for 48 h. [47]

5.1.7 Mechanical studies

The developed hydrogels were thoroughly characterized by cyclic compression, repetitive stress relaxation and repetitive creep studies. The samples for the mechanical studies were molded into cylindrical shape (diameter= 13.7 mm, height=16.5 mm, stress area= 147.76 mm). A 30 mm flat probe was used for conducting the studies. All the studies were conducted for 10 cycles at a speed of 1 mm/sec. [48]

5.1.8 Electrical studies

The electrical properties of the developed hydrogels were studied using an in-house built I-V analyzer and an impedance analyzer. The hydrogels were made in cylindrical molds. Gold plated copper electrodes were used for the electrical characterization of the hydrogels. [49]

5.1.9 Thermal studies

The thermal measurements were done using DSC 200 F3 Maia (Netzsch Instruments Limited, Germany) instrument. The thermal properties associated with the different thermal events were determined by heating the samples and subsequently cooling the samples in the heating range of 20 ^{o}C to 200 ^{o}C. The rate of heating or cooling was 5 ^{o}C/min. The experiments were conducted under inert nitrogen environment.

5.1.10 In vitro cytocompatibility studies

The *in vitro* cytocompatibility of the samples were analyzed using HaCat (Human Keratinocytes) cells by leachant extraction method. In brief, the samples were powdered in a mortar and pestle after freezing in liquid nitrogen. 1 g of the powdered samples were immersed in 10 ml of PBS (pH 7.2) at 37 ^{o}C and incubated in a shaker incubator for 24 h. The extracts were filtered using a microfilter (0.22 µm). 10 µl of the filtered extract was added to a 96 well plate previously seeded

with $1x10^4$ cells/well and subsequently incubated for 24 h in a CO_2 incubator. Dulbecco's Modified Eagle Medium (DMEM) – 10 % Fetal Bovine Serum (FBS) was used as the cell culture medium. The cell viability was calculated using MTT assay method. All the assays were done in triplicates.

5.1.11 Drug Kinetics studies

The drug kinetic study was done on the prepared pHEMA-MC hydrogel system in order to see the drug delivering efficiency of the hydrogels. This study was done using 25 mg of the dried powder of insulin, which was mixed with hydrogels during their preparations itself. The prepared hydrogels were then immersed in 40 ml of PBS, pH 7.4 and were kept at 37 °C in a shaker incubator for mild shaking. The study was carried out for 8 h, and at different predetermined time intervals 1 ml of the solution was withdrawn from the release medium with addition of equal volume of the prepared PBS solution into the release medium.

5.2 RESULT AND DISCUSSIONS

5.2.1 Preparation of the Hydrogels

The hydrogels, containing various proportions of MC, were prepared by free radical polymerization of HEMA. The free radical polymerization was initiated using APS-TEMED redox pair initiator. The percentage monomer conversion of HM1 was found to be 97 % ± 2%. No attempts were made to cross-link MC. These types of hydrogels are often regarded as semi-IPN polymeric hydrogels [50]. All the hydrogels were white in color. The white color of the pHEMA hydrogels have been attributed to the heterogeneous precipitation of pHEMA during bulk polymerization. HEMA is a water-soluble monomer but during bulk polymerization there is an increase in the hydrophobicity of the polymer, which in turn, results in the change in the solubility parameter. Usually pHEMA gels are transparent in nature if they are prepared in an aqueous

environment containing lower proportion of water. Increase in the water content above 45% has been reported to induce phase separation of the polymer (a heterogenous phenomenon). This makes the hydrogel to appear as milky white opaque polymeric constructs [51]. The whiteness of the hydrogels increased with the increase in the MC content. The apparent firmness of the hydrogels was lower when the MC content was higher. There was a corresponding increase in the stickiness of the hydrogels when the proportion of MC was increased. The pictographs of the hydrogels have been shown in the Figure 1. The hydrogels were soothing to touch and did not have any odor.

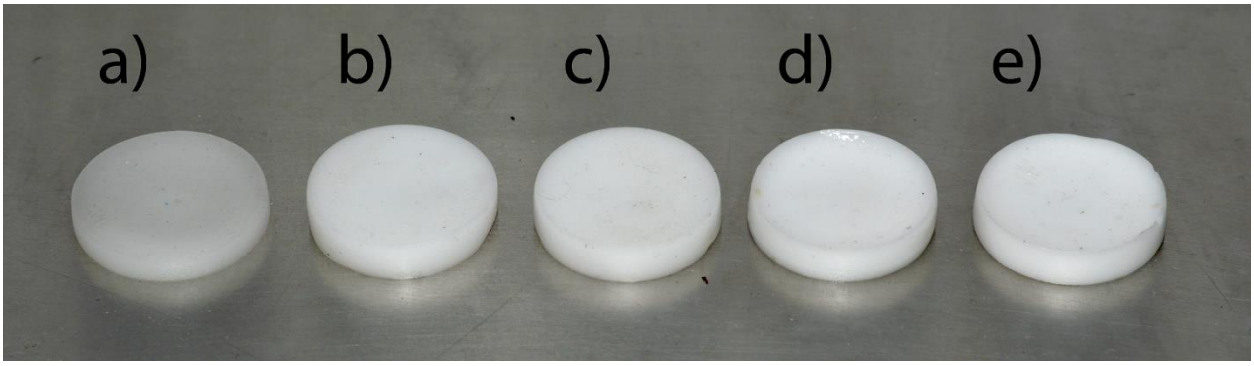

Figure 5.1: Pictographs of the prepared hydrogels: a) HM1; b) HM2; c) HM3; d) HM4; e) HM5

5.2.2 Degree of polymerization

Flory-Rehner theory is based on the equilibrium swelling theory that allows the determination of the degree of polymerization based on the swelling limits. This theory is based on the principle that a polymer will absorb its neighboring solvent until the solvent chemical potentials of the polymer are equal both inside and outside. Table 2 represents the key parameters that have been used to solve the equation. Average molecular weight (M_c) after cross-linking was found to be 14.07 ± 0.32 g/mol and degree of polymerization (X) was 9.28 ± 0.16.

The Flory parameter (χ_1) is based on the polymer-solvent interaction and is a function of both temperature and concentrations. χ_1 is often determined empirically. In hydrogel system, such as, pHEMA where the hydrogen bonding is significant, [52] [53]this empirically calculated χ_1 value becomes inaccurate and the calculation of degree of polymerization stands only as an approximation.

Table 5.2: Parameters used for the determination of the average molecular weight between polymer cross-links and the cross-linking density

Parameter	Value
M (primary molecular mass)	130.14g/mol
$\bar{v}$ **(hydrogel specific volume)**	0.891 cm^3/g
V (molar volume of water)	18 cm^3/mol
$v_{2,s}$ **(polymer volume fraction post-swelling)**	experimental
ρ_2 **(density of hydrogel)**	1.12 g/cm^3
ρ_1 **(density of water)**	0.998 g/cm^3
χ_1 **(Flory solvent-polymer interaction term)**	0.60 (approx.)

5.2.3 Microscopic Studies

The microstructure of HM1 showed presence of interlocked globular structures (Figure 2). Similar kind of observation has been reported by A. Das *et al.* (2011) while synthesizing acrylate based-hydrogels [54]. Such kind of structural arrangement may be explained by the presence of hydrophobic backbone of pHEMA and hydrophilic hydroxyl groups. This imparts an ampiphilic character to pHEMA. Hence, during the preparation of the hydrogels, the hydrophobic domains try to form spherical droplets, such that, the hydrophobic domains form the core of the droplets. The hydrophilic hydroxyl groups appear onto the surface of these droplets. The fluorescent micrograph of the hydrogels (Figure 3) suggested a hydrophobic nature of the spherical droplets. Incorporation of MC into the pHEMA matrices showed relatively distant globular particles in HM2, HM3 and HM4, respectively. A further increase in the MC content in HM5 resulted in the

formation of a bicontinuous biphasic formulation. The bicontinuous formulations are categorized by the presence of both the phases as continuum phase.

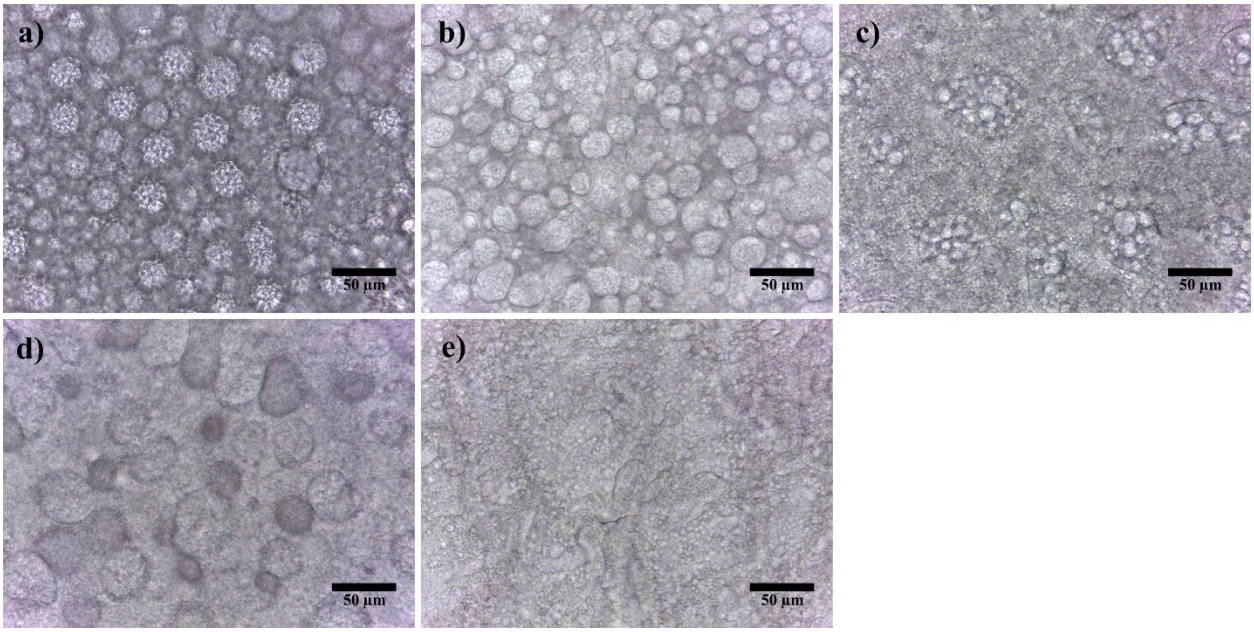

Figure 5.2: Bright field micrographs of the hydrogels. a) HM1, b) HM2, c) HM3, d) HM4, and e) HM5

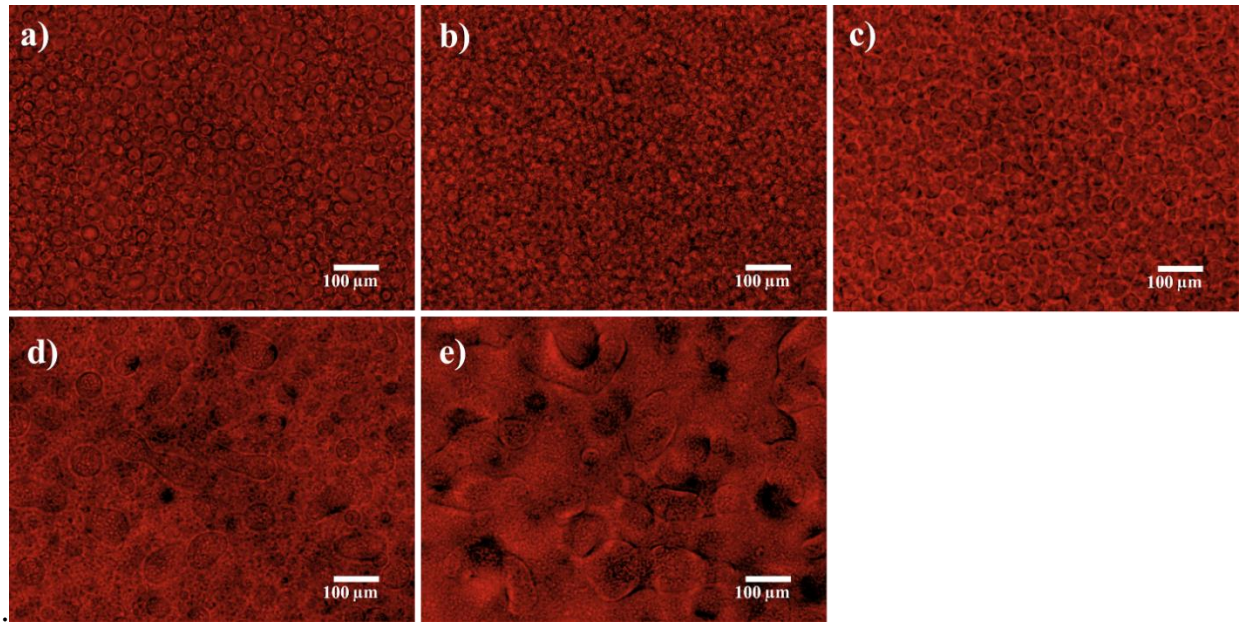

Figure 5.3: Fluorescent micrographs of the hydrogels. a) HM1, b) HM2, c) HM3, d) HM4, and e) HM5

5.2.4 XRD studies

The XRD profiles of the hydrogels were found to be similar (Figure 4a). A major broad peak at 19^o 2θ followed by two broad peaks at nearly 31^o and 43^o 2θ, respectively, was observed in all the hydrogels. Apart from these prominent peaks, a shoulder peak at ~12^o 2θ was also observed. Absence of any sharp peaks in the profile was an indicative of predominant amorphous nature of the hydrogels. The full width at half maximum (FWHM) of the peak at nearly 19^o 2θ was calculated to have an understanding about the variation in the crystallinity of the hydrogel matrices. The FWHM of the hydrogels were in the order of HM1≈HM3>HM4>HM2>HM5. FWHM has been reported to be inversely related to the crystallinity of the formulations [55]. The results suggested that the incorporation of MC into the pHEMA matrix resulted in the increased crystallinity of the HM2. A further increase in the MC content resulted in the increase in the amorphosity of HM3. Thereafter, an increase in the MC content resulted in the subsequent increase in the crystallinity of the hydrogels.

5.2.5 FTIR spectroscopic studies

FTIR spectra of the raw materials and the hydrogels have been shown in Figure 4b. MC showed a small hump-like structure at ~2900 cm^{-1} because of CH stretching, associated with the ring methane hydrogen atoms [56]. The FTIR spectrum of MC showed peaks at ~1100 cm^{-1} and 1040 cm^{-1}, corresponding to CO stretching vibrations in the polysaccharide skeleton. [40] FTIR spectrum of HEMA showed characteristic peaks of stretching vibrations of OH, CH and CO at ~3500 cm^{-1}, ~3000 cm^{-1} and ~1735 cm^{-1}, respectively [57]. These peaks were conserved in the hydrogels, but their intensity was altered. This indicated that there was a change in the micro-environment of the functional groups. The result can be correlated with the XRD studies, which

indicated changes in the crystallinity of the hydrogels as the composition was varied. The OH absorption bond was found to be broadened in the formulations. This may be because of the strong hydrogen bonding between pHEMA and MC [58].

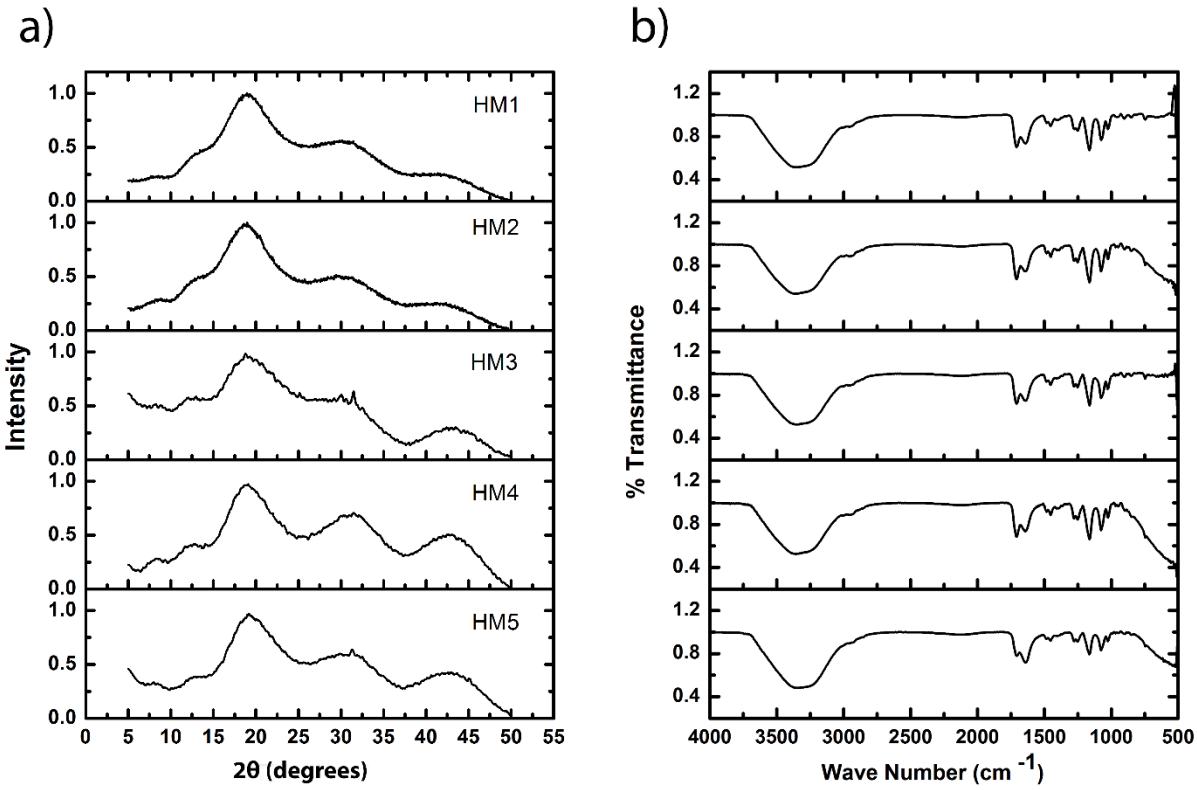

Figure 5.4: a) XRD and b) FTIR graphs of the hydrogels

5.2.6 Swelling studies

The swelling properties of the hydrogels were tested at three different temperatures using buffers of either pH 1.2, 7 or 9 (Figure 5). An increase in the MC content resulted in the increase in the swelling capability of the hydrogels. This trend was observed under all the temperatures. The degree of swelling of the hydrogels at different pHs (varying the temperature) suggested that the degree of swelling was lower at pH 1.2. The degree of swelling increased when the pH of the

swelling media was increased to 7. A further increase in the pH to 9 resulted in a corresponding decrease in the percentage swelling. This observation may be explained by the swelling/dissolution property of MC. The cellulose derivatives are usually soluble at higher pHs. At pH 1.2, the absorption of the buffer was lower since MC is poorly hydrated at lower pHs. An increase in the pH to 7 resulted in the increased hydrophilicity of MC, which in turn, resulted in the increase in the swelling of the hydrogels. A further increase in the pH to 9 resulted in the quick hydration and dissolution of the MC. This resulted in the diffusion of the MC out of the hydrogel matrix, thereby causing a decrease in the percentage swelling because of the elastic reconciliation of the pHEMA matrix towards the core.

As the temperature of the swelling media was increased from 4 ^{o}C to 37 ^{o}C, a corresponding decrease in the percentage swelling of the hydrogels were observed. This observation may be related to the temperature sensitive property of MC. The aqueous solutions of MC undergo an increase in the viscosity as the temperature is increased [59], which may result in the formation of a gelled structure at 37 ^{o}C. The formation of the reversible gelled structure at higher temperatures resulted in the shrinkage of the MC phase with a corresponding decrease in the hydrophilicity. The reduction in the hydrophilicity of MC may explain the decrease in the percentage swelling of the hydrogels at higher temperatures.

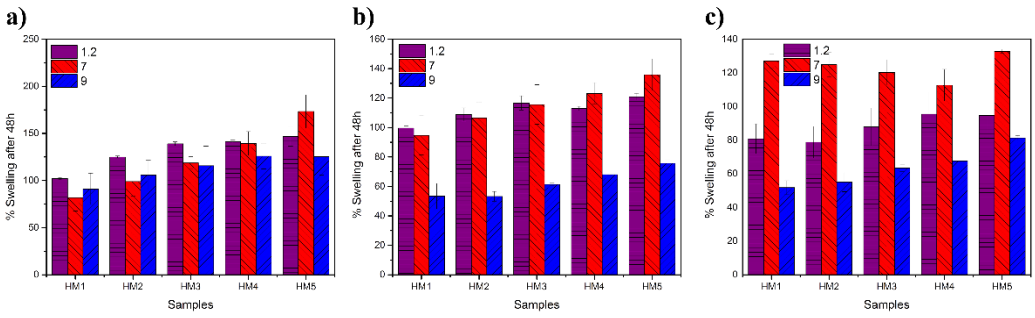

Figure 5.5: Swelling properties of the hydrogels. a) 4 °C, b) 25 °C and c) 37 °C

5.2.7 Mechanical testing

The firmness of the hydrogels was predicted from the stress relaxation study by determining D_{20} values (Figure 6a). This parameter is used often in food industries to estimate the firmness of the semi-solid food products. [60] D_{20} value is defined as the distance moved by the probe to attain a 20 g force. Longer the distance moved by the probe to attain a said force indicates softer nature of the hydrogels. In the present case, highest D_{20} value was observed in HM1 followed by HM4, HM5, HM3 and HM2, respectively. This suggested that the firmness of the pHEMA hydrogel (HM1) was lowest. As the concentration of the MC was increased in HM2 to HM4, there was a corresponding increase in the D_{20} value. A subsequent increase in the MC content in HM5 resulted in the decrease in the D_{20} value. The observation suggested that an increase in the MC content resulted in the decrease in the firmness of the hydrogels with the exception of HM5. This exception may be explained by the change in the microstructural arrangement of the pHEMA and MC phases. The hydrogels showed a decrease in the D_{20} value when the hydrogels were subjected to cyclic stress relaxation studies. This may be explained by the bulk work-hardening of the hydrogels when repetitive stress relaxation study was performed.

Stress relaxation (SR) study of the hydrogels was calculated for 10 cycles. The results have been shown in Figure 6b. The percent stress relaxation (%SR) of HM1 was found to be lowest. The increase in the MC content resulted in the corresponding decrease in the %SR values. %SR of the hydrogels showed an initial decrease followed by a base stationary phase as the hydrogels were subjected to repetitive SR studies. The results indicated an increase in the elastic component of the hydrogels when subjected to repetitive SR studies. %SR is a measure of viscoelastic property of the material. A %SR of 100 % suggests fluid nature of the formulation, whereas, a %SR of 0 % is an indicator of an elastic material. The hydrogels showed percent stress relaxation in between 0 %

and 100 %. This is an indicative of viscoelastic nature of the prepared hydrogels. Amongst all the hydrogels, HM1 showed highest elastic nature, that is, the %SR was lowest in HM1. In general, addition of MC resulted in the increase in the fluid nature of the hydrogels. Amongst the MC containing hydrogels, the %SR was found to be in the order of HM2>HM3>HM4≈HM5. This indicated a decrease in the elastic nature with the increase in the MC content.

Cyclic creep studies were conducted to have an understanding about the variation in the long-term viscoelastic property (creep compliance, creep indentation and percent recovery) of the hydrogels (Figure 6c-h) [61]. The viscosity of HM1 was highest amongst all the hydrogels. Incorporation of MC into the hydrogel structure resulted in the decrease in the viscosity in HM2. An increase in the MC concentration (HM2 to HM4) resulted in the increase in the viscous component of the hydrogels. Thereafter, a further increase of MC content resulted in a corresponding decrease in the initial viscous component. The initial viscosity was in the order of HM1>HM4>HM3≈HM5>HM2. On the contrary, an increase in the MC content resulted in the decrease in the creep compliance. The initial creep compliance value was in the order of HM2>HM3>HM4>HM5>HM1. Creep compliance provides information about the ability of a material to undergo immediate recovery to its original shape when an applied stress is removed from the formulations [61]. A formulation having a higher elastic component usually has a lower viscous component. The viscous and the creep compliance values of the prepared hydrogels were in support of each other. Further, when the hydrogels were subjected to repetitive creep cycles, an increase in the viscosity with a corresponding decrease in the creep compliance was observed. The recovery of the hydrogels from the deformation, when the applied stress is withdrawn, provides information about the elastic component [61]. If a material is elastic in nature, a 100% recovery is a usual phenomenon. On the contrary, a partial recovery of the deformation of the formulations

was observed. This is because of the loss of the viscous component during the creep phase. The hydrogels, in general, showed an increase in the percent recovery during the initial cycles which attained a plateau phase during the later phase of the cycles. This indicated a decrease in the viscous component with a corresponding increase in the elastic component as the hydrogels were subjected to repetitive creep studies. Further, during the later phase of the creep cycles, a constant recovery was seen. This indicated complete loss of the viscous component. The recovery results are in support of the results obtained from the creep studies (viscosity and creep compliance). The percent recovery at the end of the 10^{th} cycle (final cycle) was in the order of HM2>HM3≈HM4>HM1>HM5.

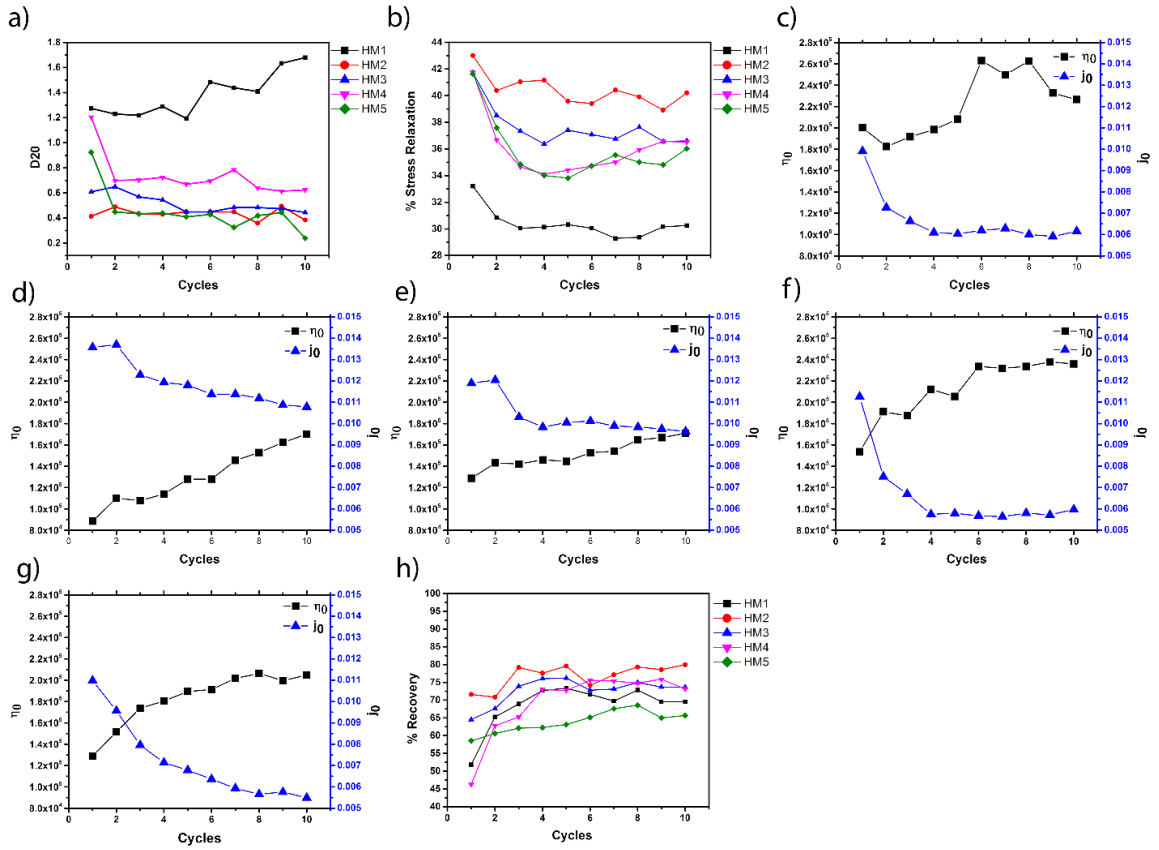

Figure 5.6: Mechanical properties of the hydrogels. a) D20; b) Cyclic Stress Relaxation; Cyclic creep study of: c) HM1, d) HM2, e) HM3, f) HM4, g) HM5; and, h) Creep recovery.

5.2.8 Conductivity studies

I-V characteristics of the hydrogels were determined using a sinusoidal signal of 10 KHz (Figure 7). For the analysis, a variable current (I_{rms}=10 mA to 300 mA) was passed through the hydrogels and the corresponding voltage drop across the hydrogel samples were measured. A sinusoidal signal was used for the analysis because the I-V characteristics measured using DC current are affected with the polarization of the electrode-sample interface. [49] This results in the erroneous measurement of the I-V characteristics. To avoid this phenomenon, a conscious attempt was made to record the I-V characteristics at 10 KHz. The hydrogels showed a linear I-V profile. This is an indicative of the resistive dominant behavior of the hydrogels. The slope of the I-V profile of the hydrogels provides information about the resistive component of the hydrogels. The slope of the hydrogels was in the order of HM2>>HM3>HM4>HM1>HM5. The results indicate that the incorporation of MC into the hydrogel matrix resulted in the increase in the resistive component of HM2. A further increase in the MC content resulted in the subsequent decrease in the resistive component of the hydrogels. This result may be explained by the changes in the microarchitecture of the hydrogels as the MC content was increased. An increase in the MC content showed an increase in the size of the globular dispersed droplets, which formed biphasic architecture at the highest MC concentration. An increase in the droplet size resulted in the reduction of the grain boundary resistive effect which could be manifested from the I-V profiles of the hydrogels.

The conductivity of the hydrogels was measured in the frequency range of 200 Hz- 15 kHz. Incorporation of MC into the pHEMA matrix resulted in the marked decrease in the conductivity of the hydrogel. Subsequent increase in the MC content resulted in the increase in the conductivity. The conductivity profile of the hydrogels suggested capacitive dominant nature, characterized by lower conductivity at lower frequencies and a higher conductivity at higher frequencies. But the I-

V characteristics of the hydrogels showed a linear profile indicating a resistive dominant character of the hydrogels. From the above observations, it may be concluded that the capacitive dominant nature, as observed from the conductivity profile, was mainly because of the electrode-sample interface polarization. [49]

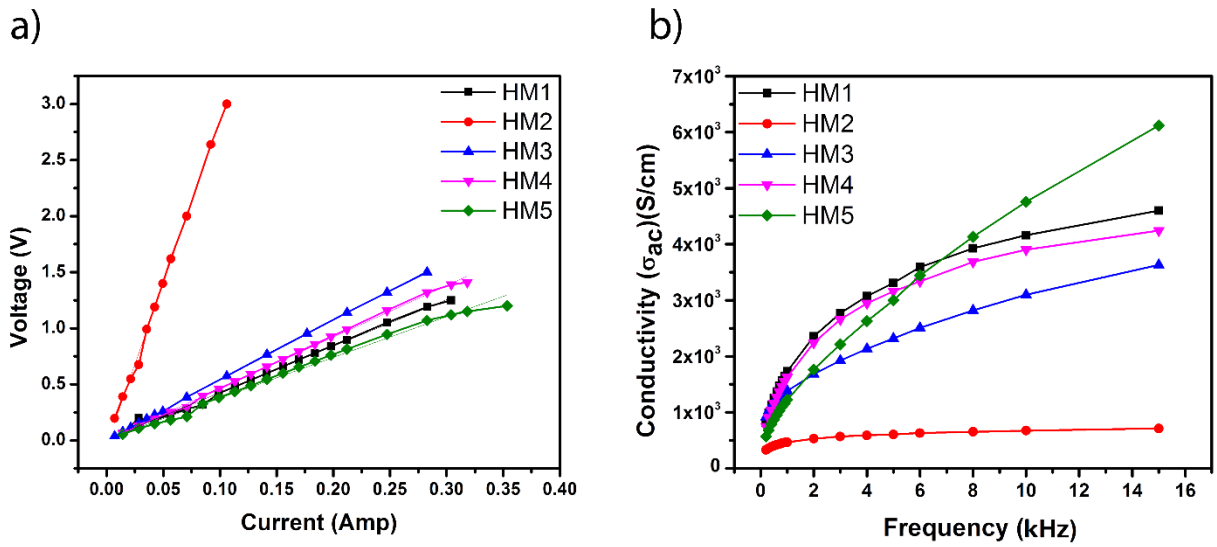

Figure 5.7: Electrical properties of the hydrogels. a) I-V characteristics; and b) Conductivity

5.2.9 Thermal studies

HM1, HM3 and HM5 were selected as the representative samples for the thermal analysis (Figure 8). All the hydrogels showed a broad endothermic peak, with a central peak position of nearly 90 ^{o}C. The broad endothermic peak during the heating cycle was because of the evaporation of the moisture content present in the hydrogel matrices. Increase in the MC concentration resulted in the shifting of the peak position of the endothermic peak towards the higher temperature. The change in the enthalpy and the entropy were calculated during the evaporation of the moisture. The result suggested that the change in the enthalpy and the entropy were highest in HM1 (control). Incorporation of MC resulted in decrease in these values. The results suggested that the moisture

retention capacity of hydrogels were higher when the concentration of the MC was lower. The cooling endotherm did not show presence of any peaks.

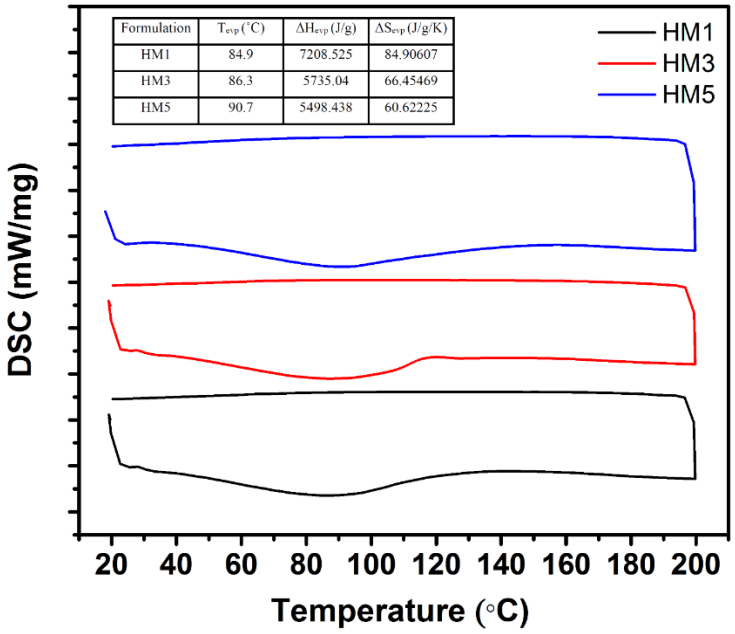

Figure 5.8: Thermal studies of HM1, HM3, HM5

5.2.10 *In vitro* cytocompatibility studies

The *in vitro* cytocompatibility of the hydrogels was analyzed using HaCat cells (Figure 9). Since both pHEMA and MC are well-known biocompatible material, the cell viability index for all the samples were found to be within acceptable biocompatible range. The results showed that HM2 and HM3 had better cell viability index than the control (HM1), whereas, HM4 and HM5 showed slightly lower cell viability index. In gist, incorporation of MC in lower proportions improved the cell viability. Subsequent increase in the MC content resulted in the decrease in the relative cell viability. Another interesting observation is that few cells turned into spheroids in all the samples (Figure 10). Thirumala *et al.* (2013) also reported similar observations using adipose tissue derived

stem cells in the presence of MC [62]. This may explain the reduced cell viability index with the increase in the MC concentration.

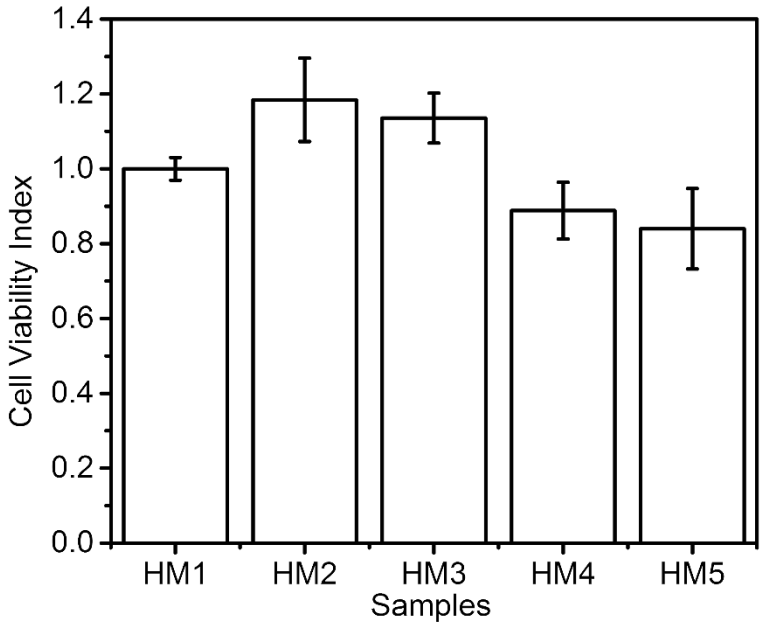

Figure 5.9: In vitro cytocompatibility study of the hydrogels

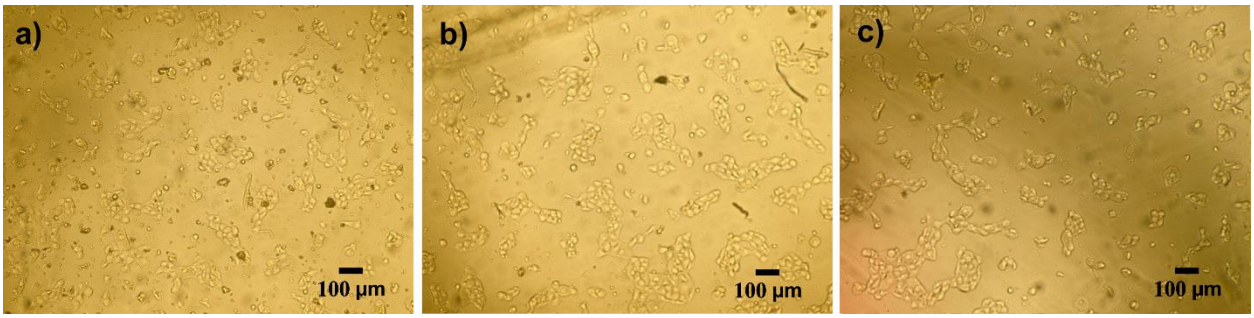

Figure 5.10: In vitro cytocompatibility micrographs of the hydrogels

5.2.11 Drug Kinetics studies

The drug kinetic studies was done by taking HM1, HM3 and HM5 as the representative samples. Fig. 5.11 shows the drug kinetic studies of the hydrogels using insulin. All the hydrogels showed drug release percentage of approximately 45-55%. HM3 which contains hydrogel having MC in 1% concentration showed a bit less drug release in compared to the control sample HM1. On the other hand, HM5 showed a better drug release profile than the control samples, thereby showing that with the increase in the methyl cellulose content the drug release profile is increasing. This may be correlated with the microstructure of the hydrogels that were observed previously. It may be due to the formation of a biphasic continuous phase in the hydrogels having higher MC content, that these hydrogels are showing better drug release.

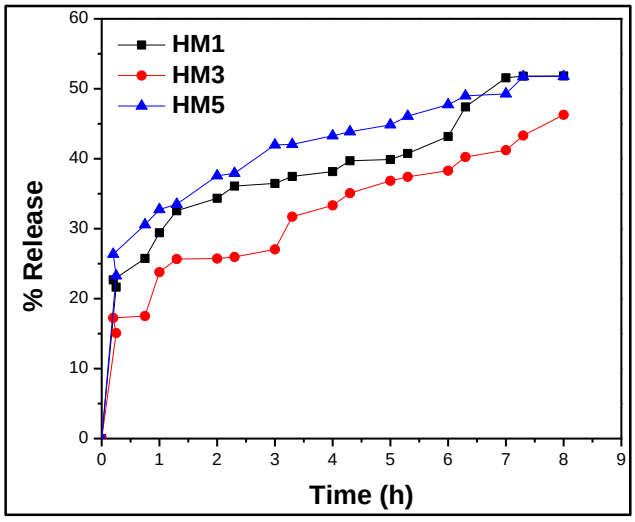

Figure 5.11 Drug Kinetics study using Insulin

5.3 CONCLUSION

The current study reports the successful development of novel dual environment sensitive acrylate based-hydrogels. The hydrogels were prepared as semi-IPN networks of pHEMA and MC. The microstructure of the hydrogels showed globular structures of pHEMA which formed self-assembled interlocked structures of 3D-polymer network. Incorporation of the MC resulted in the increase in the interglobular distance of the pHEMA globules. When the MC concentration was highest, the globular structures were completely eradicated. Instead, a bicontinuous structure was observed. Hence, it was expected that the properties of HM5 would vary from the normal trend of the properties of the other MC containing hydrogels. The mechanical studies suggested viscoelastic nature of the hydrogels. When the hydrogels were subjected to repetitive mechanical stress, it was observed that the viscous component of the hydrogels was lost quickly. The thermal studies suggested improved moisture-retention capacity of the MC containing hydrogels. The electrical properties of the hydrogels suggested resistive dominant nature of the hydrogels.

6 CONCLUSION

The current study therefore successfully showed the use of lens protein crystallins for tissue engineering applications as well as for protein drug delivery strategies. It was proposed that due to the angiogenic as well as neuroprotective role of these proteins, it can be possibly used for tissue engineering purposes and also with its role as a molecular chaperone, this protein can stabilize other proteins and thus helps in the suppression of their aggregation. Also it was proposed that may be the chaperone properties of these lens protein can be utilized during the protein drug delivery strategies and thus the proteins can be prevented from getting aggregated. The first objective of using these proteins for tissue engineering purposes was fulfilled by making a electrospin nanofibers out of these proteins and thus seeing its biocompatibility with the cells. This was for the first time these proteins were tried to be electrospun and it was found that after electrospinning these proteins are turning into amyloids and thus are showing amyloid like characteristics. Further characterizations are required to confirm the nanofibers formed to be the amyloids only.

The second objective of the study was completed by making stimuli-responsive hydrogels as a model system for the controlled drug delivery of the proteins. The dual environment responsive semi-interpenetrating hydrogels were prepared successfully by using pHEMA and MC. The microstructures of the hydrogels prepared showed distinct interlocked globular structures which was turning into biphasic continuous phase as the content of the methyl cellulose was increased. Thus it was believed that the sample containing the higher MC content will show results different from the other methyl cellulose containing hydrogels. Also to see if the hydrogels are releasing drugs in an efficient way, the drug kinetics study was done and it was shown that after 8h

approximately 60% of the drugs got released. Since the system was proposed to be used for protein drug delivery, insulin drug was used.

7 FUTURE ASPECTS

- The electrospinning of these lens crystallin proteins that were optimized using other polymers, such as, PEO, PVA etc. in presence of small amount of denaturants can be studied in detail in future and a comparison can be done between the different fibers that can be made.
- The electrospun fibers that were made by dissolving the lyophilized lens protein powder in TFA showed amyloid like characteristics this can be confirmed by doing the ThT fluorescence study.
- The chaperone activity of these lens proteins that was supposed to be utilized for protein drug delivery strategies need to be studied in detail. The protein should be delivered both in the presence as well as in the absence of these lens crystallins and how these proteins are helping in stabilizing the structures of the proteins inside the hydrogel system need to be studied.

8 RESEARCH OUTPUT

Published a paper titled "*Synthesis and characterization of novel dual-environment responsive hydrogels of 2-hydroxyethyl methacrylate and methyl cellulose"* in the journal Designed Monomers and Polymers, DOI: 10.1080/15685551.2015.1012626

9 REFERENCES

[1] J. J. Harding, Biochemistry of the Eye, Chapman \& Hall Medical, 1997.

[2] P. J. Groenen, K. B. Merck, W. W. Jong and H. Bloemendal, "Structure and Modifications of the Junior Chaperone α-Crystallin," *European Journal of Biochemistry,* vol. 225, no. 1, pp. 1-19, 1994.

[3] J. Horwitz, "Alpha-crystallin can function as a molecular chaperone," *Proceedings of the National Academy of Sciences,* vol. 89, no. 21, pp. 10449-10453, 1992.

[4] C. Zhang, P. Gehlbach, C. Gongora, M. Cano, R. Fariss, S. Hose, A. Nath, W. R. Green, M. F. Goldberg, J. S. Zigler and others, "A potential role for β-and γ-crystallins in the vascular remodeling of the eye," *Developmental dynamics,* vol. 234, no. 1, pp. 36-47, 2005.

[5] H. Ecroyd and J. A. Carver, "Crystallin proteins and amyloid fibrils," *Cellular and Molecular Life Sciences,* vol. 66, no. 1, pp. 62-81, 2009.

[6] O. Wichterle and D. Lim, "Hydrophilic gels for biological use," 1960.

[7] H. Trieu and S. Qutubuddin, "Poly (vinyl alcohol) hydrogels: 2. Effects of processing parameters on structure and properties," *Polymer,* vol. 36, no. 13, pp. 2531-2539, 1995.

[8] C. T. Mörner, "Untersuchung der Proteïnsubstanzen in den leichtbrechenden Medien des Auges I.," *Zeitschrift für physiologische Chemie,* vol. 18, no. 1, pp. 61-106, 1894.

[9] D. C. Wood, L. Massi and E. L. Solomon, "The isolation, crystallization, and properties of proteins from rabbit eye lens," *Journal of Biological Chemistry,* vol. 234, no. 2, pp. 329-334, 1959.

[10] A. Dimberg, S. Rylova, L. C. Dieterich, A.-K. Olsson, P. Schiller, C. Wikner, S. Bohman, J. Botling, A. Lukinius, E. F. Wawrousek and others, "αB-crystallin promotes tumor angiogenesis by increasing vascular survival during tube morphogenesis," *Blood,* vol. 111, no. 4, pp. 2015-2023, 2008.

[11] S. Kase, S. He, S. Sonoda, M. Kitamura, C. Spee, E. Wawrousek, S. J. Ryan, R. Kannan and D. R. Hinton, "αB-crystallin regulation of angiogenesis by modulation of VEGF," *Blood,* vol. 115, no. 16, pp. 3398-3406, 2010.

[12] J. G. Masilamoni, E. P. Jesudason, S. N. Bharathi and R. Jayakumar, "The protective effect of α-crystallin against acute inflammation in mice," *Biochimica et Biophysica Acta (BBA)-Molecular Basis of Disease,* vol. 1740, no. 3, pp. 411-420, 2005.

[13] J. G. Masilamoni, S. Vignesh, R. Kirubagaran, E. P. Jesudason and R. Jayakumar, "The neuroprotective efficacy of α-crystallin against acute inflammation in mice," *Brain research bulletin,* vol. 67, no. 3, pp. 235-241, 2005.

[14] J. Masilamoni, E. Jesudason, B. Baben, C. E. Jebaraj, S. Dhandayuthapani and R. Jayakumar, "Molecular chaperone α-crystallin prevents detrimental effects of neuroinflammation," *Biochimica et Biophysica Acta (BBA)-Molecular Basis of Disease,* vol. 1762, no. 3, pp. 284-293, 2006.

[15] J. M. van Noort, M. Bsibsi, P. Nacken, W. H. Gerritsen and S. Amor, "The link between small heat shock proteins and the immune system," *The international journal of biochemistry \& cell biology,* vol. 44, no. 10, pp. 1670-1679, 2012.

[16] S. S. Ousman, B. H. Tomooka, J. M. Van Noort, E. F. Wawrousek, K. O'Conner, D. A. Hafler, R. A. Sobel, W. H. Robinson and L. Steinman, "Protective and therapeutic role for αB-crystallin in autoimmune demyelination," *Nature,* vol. 448, no. 7152, pp. 474-479, 2007.

[17] P. G. Sreekumar, R. Kannan, M. Kitamura, C. Spee, E. Barron, S. J. Ryan and D. R. Hinton, "αB crystallin is apically secreted within exosomes by polarized human retinal pigment epithelium and provides neuroprotection to adjacent cells," *PLoS One,* vol. 5, no. 10, p. e12578, 2010.

[18] J. A. Carver and R. A. Lindner, "NMR spectroscopy of α-crystallin. Insights into the structure, interactions and chaperone action of small heat-shock proteins," *International journal of biological macromolecules,* vol. 22, no. 3, pp. 197-209, 1998.

[19] J. A. Carver, R. A. Lindner, C. Lyon, D. Canet, H. Hernandez, C. M. Dobson and C. Redfield, "The interaction of the molecular chaperone α-crystallin with unfolding α-lactalbumin: a structural and kinetic spectroscopic study," *Journal of molecular biology,* vol. 318, no. 3, pp. 815-827, 2002.

[20] M. M. Bradford, "A rapid and sensitive method for the quantitation of microgram quantities of protein utilizing the principle of protein-dye binding," *Analytical biochemistry,* vol. 72, no. 1, pp. 248-254, 1976.

[21] U. K. Laemmli and others, "Cleavage of structural proteins during the assembly of the head of bacteriophage T4," *nature,* vol. 227, no. 5259, pp. 680-685, 1970.

[22] D. M. Byler and H. Susi, "Examination of the secondary structure of proteins by deconvolved FTIR spectra," *Biopolymers,* vol. 25, no. 3, pp. 469-487, 1986.

[23] T. Rasmussen, M. van de Weert, W. Jiskoot and M. R. Kasimova, "Thermal and acid denaturation of bovine lens α-crystallin," *Proteins: Structure, Function, and Bioinformatics,* vol. 79, no. 6, pp. 1747-1758, 2011.

[24] H. Li, C. Li, Q. Lu, T. Su, T. Ke, D. W.-C. Li, M. Yuan, J. Liu, X. Ren, Z. Zhang and others, "Cataract mutation P20S of αB-crystallin impairs chaperone activity of αA-crystallin and induces apoptosis of human lens epithelial cells," *Biochimica et Biophysica Acta (BBA)-Molecular Basis of Disease,* vol. 1782, no. 5, pp. 303-309, 2008.

[25] N. H. Mueller, D. A. Ammar and J. M. Petrash, "Cell penetration peptides for enhanced entry of αB-crystallin into lens cells," *Investigative ophthalmology & visual science,* vol. 54, no. 1, pp. 2-8, 2013.

[26] S. Krimm and J. Bandekar, "Vibrational spectroscopy and conformation of peptides, polypeptides, and proteins," *Advances in protein chemistry,* vol. 38, pp. 181-364, 1986.

[27] W. K. Surewicz, H. H. Mantsch and D. Chapman, "Determination of protein secondary structure by Fourier transform infrared spectroscopy: a critical assessment," *Biochemistry,* vol. 32, no. 2, pp. 389-394, 1993.

[28] H. Susi and D. M. Byler, "Fourier deconvolution of the amide I Raman band of proteins as related to conformation," *Applied Spectroscopy,* vol. 42, no. 5, pp. 819-826, 1988.

[29] P. Garidel and H. Schott, "Fourier-transform midinfrared spectroscopy for analysis and screening of liquid protein formulations part. 2: detailed analysis and applications," *BioProcess Int,* vol. 4, no. 6, pp. 48-55, 2006.

[30] H. Susi and D. M. Byler, "[13] Resolution-enhanced fourier transform infrared spectroscopy of enzymes," *Methods in enzymology,* vol. 130, pp. 290-311, 1986.

[31] J. Bandekar, "Amide modes and protein conformation," *Biochimica et Biophysica Acta (BBA)-Protein Structure and Molecular Enzymology,* vol. 1120, no. 2, pp. 123-143, 1992.

[32] A. Dong, P. Huang and W. S. Caughey, "Protein secondary structures in water from second-derivative amide I infrared spectra," *Biochemistry,* vol. 29, no. 13, pp. 3303-3308, 1990.

[33] O. P. Lamba, D. Borchman, S. Sinha, J. Shah, V. Renugopalakrishnan and M. Yappert, "Estimation of the secondary structure and conformation of bovine lens crystallins by infrared spectroscopy: quantitative analysis and resolution by Fourier self-deconvolution and

curve fit," *Biochimica et Biophysica Acta (BBA)-Protein Structure and Molecular Enzymology*, vol. 1163, no. 2, pp. 113-123, 1993.

[34] J. T. Pelton and L. R. McLean, "Spectroscopic methods for analysis of protein secondary structure," *Analytical biochemistry,* vol. 277, no. 2, pp. 167-176, 2000.

[35] W. K. Surewicz and H. H. Mantsch, "New insight into protein secondary structure from resolution-enhanced infrared spectra," *Biochimica et Biophysica Acta (BBA)-Protein Structure and Molecular Enzymology*, vol. 952, pp. 115-130, 1988.

[36] Y. N. Chirgadze, O. Fedorov and N. Trushina, "Estimation of amino acid residue side-chain absorption in the infrared spectra of protein solutions in heavy water," *Biopolymers,* vol. 14, no. 4, pp. 679-694, 1975.

[37] A. Barth, "The infrared absorption of amino acid side chains," *Progress in biophysics and molecular biology,* vol. 74, no. 3, pp. 141-173, 2000.

[38] C. M. Johnson and A. R. Fersht, "Protein stability as a function of denaturant concentration: the thermal stability of barnase in the presence of urea," *Biochemistry,* vol. 34, no. 20, pp. 6795-6804, 1995.

[39] D. H. Correa and C. H. Ramos, "The use of circular dichroism spectroscopy to study protein folding, form and function," *African J Biochem Res,* vol. 3, no. 5, pp. 164-173, 2009.

[40] S. M. Kelly, T. J. Jess and N. C. Price, "How to study proteins by circular dichroism," *Biochimica et Biophysica Acta (BBA)-Proteins and Proteomics,* vol. 1751, no. 2, pp. 119-139, 2005.

[41] B. Raman and C. M. Rao, "Chaperone-like activity and quaternary structure of alpha-crystallin.," *Journal of Biological Chemistry,* vol. 269, no. 44, pp. 27264-27268, 1994.

[42] H. Zhang, "Electrospun poly (lactic-co-glycolic acid)/multiwalled carbon nanotubes composite scaffolds for guided bone tissue regeneration," *Journal of Bioactive and Compatible Polymers,* vol. 26, no. 4, pp. 347-362, 2011.

[43] M. F. Symmons, S. G. S. C. Buchanan, D. T. Clarke, G. Jones and N. J. Gay, "X-ray diffraction and far-UV CD studies of filaments formed by a leucine-rich repeat peptide: structural similarity to the amyloid fibrils of prions and Alzheimer's disease β-protein," *FEBS letters,* vol. 412, no. 2, pp. 397-403, 1997.

[44] J. Comyn, *Polymer science dictionary 2nd edition: Mark Alger Chapman & Hall£ 125.00. ISBN 0 412 60870 7. 628 pages+ xii*, Elsevier, 1997.

[45] G. Thakur, M. A. Naqvi, D. Rousseau, K. Pal, A. Mitra and A. Basak, "Gelatin-based emulsion gels for diffusion-controlled release applications," *Journal of Biomaterials Science, Polymer Edition,* vol. 23, no. 5, pp. 645-661, 2012.

[46] N. Peppas, P. Bures, W. Leobandung and H. Ichikawa, "Hydrogels in pharmaceutical formulations," *European journal of pharmaceutics and biopharmaceutics,* vol. 50, no. 1, pp. 27-46, 2000.

[47] S. Mallick, S. S. Sagiri, B. Behera, K. Pal and S. S. Ray, "Gelatin-based emulsion hydrogels as a matrix for controlled delivery system," *Materials and manufacturing processes,* vol. 27, no. 11, pp. 1221-1228, 2012.

[48] B. Behera, S. S. Sagiri, V. K. Singh, K. Pal and A. Anis, "Mechanical properties and delivery of drug/probiotics from starch and non-starch based novel bigels: A comparative study," *Starch-St{\"a}rke,* vol. 66, no. 9-10, pp. 865-879, 2014.

[49] V. K. Singh, A. Anis, S. Al-Zahrani, D. K. Pradhan and K. Pal, "Molecular and electrochemical impedance spectroscopic characterization of the carbopol based bigel and its application in iontophoretic delivery of antimicrobials," *Int J Electrochem Sci,* vol. 9, pp. 5049-60, 2014.

[50] J.-T. Zhang, R. Bhat and K. D. Jandt, "Temperature-sensitive PVA/PNIPAAm semi-IPN hydrogels with enhanced responsive properties," *Acta Biomaterialia,* vol. 5, no. 1, pp. 488-497, 2009.

[51] T. W. Carone, Hydrogels for central nervous system regeneration: Surface modulus and microtopographical effects on neuronal cell behavior, ProQuest, 2008.

[52] L. Brannon-Peppas and N. A. Peppas, "Time-dependent response of ionic polymer networks to pH and ionic strength changes," *International journal of pharmaceutics,* vol. 70, no. 1, pp. 53-57, 1991.

[53] A. F. Barton, CRC handbook of solubility parameters and other cohesion parameters, CRC press, 1991.

[54] A. Das, S. Ghosh and A. R. Ray, "Unveiling the self-assembly behavior of copolymers of AAc and DMAPMA in situ to form smart hydrogels displaying nanogels-within-macrogel hierarchical morphology," *Polymer,* vol. 52, no. 17, pp. 3800-3810, 2011.

[55] D. K. Shah, S. S. Sagiri, B. Behera, K. Pal and K. Pramanik, "Development of olive oil based organogels using sorbitan monopalmitate and sorbitan monostearate: A comparative study," *Journal of applied polymer science,* vol. 129, no. 2, pp. 793-805, 2013.

[56] J.-F. Su, Z. Huang, X.-Y. Yuan, X.-Y. Wang and M. Li, "Structure and properties of carboxymethyl cellulose/soy protein isolate blend edible films crosslinked by Maillard reactions," *Carbohydrate Polymers,* vol. 79, no. 1, pp. 145-153, 2010.

[57] M. F. A. Taleb, H. A. El-Mohdy and H. A. El-Rehim, "Radiation preparation of PVA/CMC copolymers and their application in removal of dyes," *Journal of hazardous materials,* vol. 168, no. 1, pp. 68-75, 2009.

[58] E. Castillo, J. Koenig, J. Anderson and J. Lo, "Protein adsorption on hydrogels: II. Reversible and irreversible interactions between lysozyme and soft contact lens surfaces," *Biomaterials,* vol. 6, no. 5, pp. 338-345, 1985.

[59] A. Haque and E. R. Morris, "Thermogelation of methylcellulose. Part I: molecular structures and processes," *Carbohydrate Polymers,* vol. 22, no. 3, pp. 161-173, 1993.

[60] "http://www.brookfieldengineering.com/education/applications/texture-butter-margarine-spreadability.asp," Engineering, B, 2 Jan 2015. [Online].

[61] M. T. Yilmaz, S. Karaman, M. Dogan, H. Yetim and A. Kayacier, "Characterization of O/W model system meat emulsions using shear creep and creep recovery tests based on mechanical simulation models and their correlation with texture profile analysis (TPA) parameters," *Journal of Food Engineering,* vol. 108, no. 2, pp. 327-336, 2012.

[62] S. Thirumala, J. M. Gimble and R. V. Devireddy, "Methylcellulose Based Thermally Reversible Hydrogel System for Tissue Engineering Applications," *Cells,* vol. 2, no. 3, pp. 460-475, 2013.